
# ΑΛΕΞΑΝΔΡΕΙΟ ΤΕΧΝΟΛΟΓΙΚΟ ΕΚΠΑΙΔΕΥΤΙΚΟ ΙΔΡΥΜΑ ΘΕΣΣΑΛΟΝΙΚΗΣ

ΣΧΟΛΗ ΤΕΧΝΟΛΟΓΙΚΩΝ ΕΦΑΡΜΟΓΩΝ (ΣΤΕΦ)

ΤΜΗΜΑ ΜΗΧΑΝΙΚΩΝ ΑΥΤΟΜΑΤΙΣΜΟΥ

**ΒΕΛΤΙΣΤΟΣ ΕΛΕΓΧΟΣ ΥΒΡΙΔΙΚΟΥ ΟΧΗΜΑΤΟΣ ΚΥΨΕΛΗΣ ΚΑΥΣΙΜΟΥ**

Πτυχιακή εργασία

Δαμίγος Παπώτης Απόστολος Αλέξιος

**Επιβλέποντες:** Καθ. Παπαδοπούλου Σημίρα
Επ. Καθ. Υφούλης Χρήστος
Δρ. Ζιώγου Χρυσοβαλάντου

Θεσσαλονίκη, Ιούνιος 2017


# ALEXANDER TECHNOLOGICAL EDUCATIONAL INSTITUTE THESSALONIKI

## AUTOMATION ENGINEERING DEPARTMENT

**OPTIMAL CONTROL OF A FUEL CELL HYBRID ELECTRIC VEHICLE**

Bachelor Thesis

Damigos Papotis Apostolos Alexios

**Supervisors:** Prof. Papadopoulou Simira
Assist. Prof. Yfoulis Christos
Dr. Ziogou Chrysovalantou

Thessaloniki, June 2017

*Θα ήθελα να ευχαριστήσω την κ. Ζιώγου για την ανεκτίμητη καθοδήγηση και την υπέρμετρη υπομονή που έδειξε καθ' όλη την διάρκεια αυτής της διαδρομής,*

*τον κ. Υφούλη για το έναυσμα που μου παρείχε για να ασχοληθώ με το αντικείμενο και την εμπιστοσύνη που μου έδειξε,*

*την κ. Παπαδοπούλου και τον κ. Βουτετάκη για τις πολύτιμες συμβουλές τους,*

*το Εθνικό Κέντρο Έρευνας & Τεχνολογικής Ανάπτυξης*

*το τμήμα Αυτοματισμού,*

*και την οικογένειά μου για την στήριξή τους όλα αυτά τα χρόνια.*

*All models are wrong, but some are useful.  - George Box*

# Thesis Publications

The results from this thesis were presented at two conferences and one journal which is under submission.

1. A. Damigos, C. Ziogou, C. Yfoulis, S. Voutetakis and S. Papadopoulou, "Optimal Energy Distribution of a Fuel Cell Electric Vehicle," *11th Panhellenic Chemical Engineering Scientific Conference,* 25-27 May 2017, Thessaloniki, Greece

2. A. Damigos, C. Ziogou, C. Yfoulis, S. Voutetakis and S. Papadopoulou, "Optimal Energy Distribution of a Fuel Cell Electric Vehicle," *1st Workshop in Microsystems*, 20 Dec 2016, Sindos, Greece

3. A. Damigos , C. Ziogou, C. Yfoulis, S. Voutetakis and S. Papadopoulou, "Model Predictive Control Framework for a Fuel Cell Hybrid Electric Vehicle,"* *Int. Journal of Hydrogen Energy*

**Under preparation*

# Περίληψη

Η παρούσα πτυχιακή εργασία εκπονήθηκε σε συνεργασία με το Εργαστήριο Ανάπτυξης Ολοκληρωμένων Συστημάτων Διεργασιών (ΕΑΝΟΣΥΣ) του Ινστιτούτου Χημικών Διεργασιών και Ενεργειακών Πόρων (ΙΔΕΠ) στο Εθνικό Κέντρο Έρευνας και Τεχνολογικής Ανάπτυξης (ΕΚΕΤΑ).

Σκοπός αυτής της εργασίας είναι η μελέτη στρατηγικών διαχείρισης ενέργειας σε ηλεκτρικά οχήματα με κυψέλη καυσίμου, και η υλοποίηση ενός βέλτιστου προρρητικού ελεγκτή (Model Predictive Control - MPC). Το σύστημα υπό μελέτη αποτελείται από μία κυψέλη καυσίμου με μεμβράνη ανταλλαγής πρωτονίων (PEMFC), μια μπαταρία ιόντων λιθίου, έναν DC/DC μετατροπέα και έναν ηλεκτροκινητήρα συνδεδεμένο απευθείας στον άξονα μετάδοσης του οχήματος. Με την χρήση των μαθηματικών μοντέλων που διέπουν το σύστημα, μπορεί να υλοποιηθεί ένας προρρητικός ελεγκτής που θα διασφαλίζει την βέλτιστη λειτουργία του συστήματος, και ταυτόχρονα θα διατηρεί τα σημεία λειτουργίας των επιμέρους στοιχείων που το αποτελούν σε ασφαλή επίπεδα που επιμηκύνουν την διάρκεια ζωής τους. Για την επίλυση του προβλήματος βελτιστοποίησης αξιοποιήθηκε η μέθοδος του μη γραμμικού προγραμματισμού (NLP), υπό την μορφή αλγορίθμου Interior Point.

Η παρούσα πτυχιακή διαρθρώνεται σε 8 κεφάλαια. Στο κεφάλαιο 1 υπάρχει μία σύντομη επισκόπηση της εργασίας στα Ελληνικά, στη συνέχεια η εισαγωγή στα Αγγλικά (κεφάλαιο 2), η βιβλιογραφική ανασκόπηση (κεφάλαιο 3), η περιγραφή του συστήματος στο κεφάλαιο 4, το παράδειγμα του ευριστικού ελεγκτή (κεφάλαιο 5), ο βέλτιστος μη γραμμικός προρρητικός ελεγκτής στο κεφάλαιο 6 και τέλος τα συμπεράσματα (κεφάλαιο 7) και οι αναφορές στο κεφάλαιο 8.

# Abstract

This Bsc thesis was developed in collaboration with the Process Systems Design and Implementation lab (PSDI) of the Chemical Process and Energy Resources Institute (CPERI) at the Center for Research and Technology-Hellas (CERTH).

The purpose of this work is to develop a framework to study the behavior of a Fuel Cell Electric Vehicle (FCEV) and energy management strategies, and implement an optimal control theory approach in the form of a Model Predictive Controller (MPC) that governs both the power split and the operation of the FC. The studied system is comprised of a Proton Exchange Membrane Fuel Cell (PEMFC), a Li-Ion battery, a DC/DC converter and an electric motor fitted directly to the vehicle drive shaft. Using mathematical models that describe the operation of the system and its components it is possible to study its behavior under various operational scenarios and formulate advanced control techniques.

In order to solve the optimization problem the method of nonlinear programming was utilized, in the form of an Interior Point algorithm.

The thesis is structured around 8 chapters. Chapter 1 contains a brief overview of the thesis in Greek, followed by the introduction in English in chapter 2, the literature review (chapter 3), the description of the system in chapter 4, the development and functionality of the heuristics controller (chapter 5), the formulation and operation of the nonlinear model predictive controller in chapter 6, and finally the conclusions (chapter 7) and the references in chapter 8.

# Contents

# Figures

## Tables

# 1

# Σύντομη Επισκόπηση

Σκοπός αυτού του κεφαλαίου είναι να εισάγει τον αναγνώστη στον τρόπο λειτουργίας του συστήματος υπό μελέτη, καθώς και στην διαδικασία της ανάπτυξης του σχήματος ελέγχου και της βελτιστοποίησης.

## 1.1 Εισαγωγή

Με την συνεχόμενα αυξανόμενη ανησυχία για μη αναστρέψιμη κλιματική αλλαγή, γίνονται όλο και πιο ελκυστικά εναλλακτικά συστήματα μεταφοράς που είναι φιλικά προς το περιβάλλον. Τα ηλεκτρικά οχήματα κυψέλης καυσίμου ενδέχεται μελλοντικά να αποτελέσουν σημαντικό κομμάτι του τομέα της μετακίνησης. Οι κυψέλες καυσίμου παρουσιάζουν πλεονεκτήματα που τις καθιστούν ιδιαίτερα ταιριαστές για τέτοιου είδους εφαρμογές, όπως ελάχιστα κινούμενα μέρη και αθόρυβη λειτουργία. Για να μελετηθεί η συμπεριφορά του οχήματος, τα επιμέρους υποσυστήματα (μπαταρία, κυψέλη καυσίμου, ηλεκτροκινητήρας, όχημα) μοντελοποιήθηκαν σε περιβάλλον MATLAB. Για να επιτευχθεί η βέλτιστη λειτουργία του συστήματος, στόχος είναι η ελαχιστοποίηση μίας συνάρτησης κόστους που συμπεριλαμβάνει την απόκλιση της πραγματικής ροπής από την απαιτούμενη του χρήστη, αλλά και έναν όρο που καθορίζει πόση ισχύς θα παρθεί από την κυψέλη καυσίμου και πόση από την μπαταρία. Παρόμοια συστήματα [1] έχουν μελετηθεί αλλά είτε λαμβάνοντας υπόψιν μόνο την διαχείριση της ενέργειας είτε χρησιμοποιώντας γραμμικοποιημένα μοντέλα [2].

## 1.2 Μοντέλο Συστήματος

Για την μοντελοποίηση του συστήματος χρησιμοποιήθηκαν μαθηματικά μοντέλα των υποσυστημάτων που το αποτελούν (μπαταρία [3], κυψέλη καυσίμου [4], κινητήρας, όχημα), τα οποία συνδεδεμένα κατάλληλα είναι ικανά να περιγράψουν πλήρως την λειτουργία του. Από τις εισόδους του συστήματος (ροές αέρα – καυσίμου, ρεύμα μπαταρίας – κ.κ.) υπολογίζεται η κατάσταση της μπαταρίας και της κυψέλης καυσίμου, υπολογίζεται η διαθέσιμη ισχύς που τροφοδοτείται στον κινητήρα και στην συνέχεια η ροπή αυτού στο μοντέλο του οχήματος. Η κύρια πηγή ενέργειας στο σύστημα είναι η κ.κ., και η δευτερεύουσα η μπαταρία. Πιο συγκεκριμένα τα βασικά χαρακτηριστικά του συστήματος είναι τα ακόλουθα:

- Κυψέλη καυσίμου μεμβράνης ανταλλαγής πρωτονίων (PEMFC): κύρια πηγή ενέργειας, ονομαστικής ισχύος 85 kW και μέγιστη 100 kW. Η ονομαστική τάση είναι 288 Vdc με μέση αποδοτικότητα 58 %. Η λειτουργία γίνεται στους 75 °C και 3 bar πίεση.
- Μπαταρία ιόντων λιθίου: 20 Ah, 288 Vdc, 25 kW.
- Σύγχρονος κινητήρας μόνιμου μαγνήτη (PMSM): Ισχύς 100 kW και μέγιστη ροπή 256 Nm.
- Ηλεκτρονικά ισχύος: Μετατροπέας DC/DC (95% αποδοτικότητα) και αντιστροφέας.

## 1.3 Προρρητικός Έλεγχος Βασισμένος σε Μοντέλο

Προκειμένου να καλυφθούν οι λειτουργικές απαιτήσεις του συστήματος και των υποσυστημάτων που το αποτελούν, είναι αναγκαία η αξιοποίηση κάποιου είδους προηγμένου ελεγκτή, ικανού να ανταπεξέλθει σε αυτά τα ζητούμενα. Κύρια ζητούμενα είναι κάλυψη της απαιτούμενης ροπής από τον χρήστη, και η διατήρηση της κ.κ. σε κατάλληλα επίπεδα ορθής λειτουργίας. Ο προρρητικός έλεγχος θεωρείται μια δημοφιλής τεχνική προηγμένης ρύθμισης χάρη στη δυνατότητα που έχει να χειρίζεται το ελεγχόμενο σύστημα με τέτοιο τρόπο, ώστε να ικανοποιούνται πολλαπλά και μεταβαλλόμενα λειτουργικά κριτήρια, ακόμη και όταν υπάρχουν αλλαγές στα χαρακτηριστικά του ή υπόκειται σε περιορισμούς. [5]

Το σχήμα ελέγχου βασίζεται στις προρρήσεις ενός μη γραμμικού μοντέλου και έχει ως στόχο να οδηγήσει το σύστημα στη βέλτιστη περιοχή λειτουργίας. Ένα πρόβλημα βελτιστοποίησης ανοικτού βρόχου επιλύεται για έναν ορίζοντα πρόβλεψης ($T_p$), χρησιμοποιώντας την τρέχουσα κατάσταση του συστήματος ως αρχική τιμή. Από τη βελτιστοποίηση προκύπτει η ακολουθία των δράσεων ελέγχου ($u_k$.. $u_{k+Nc}$) για τον ορίζοντα ελέγχου ($T_c$), ο οποίος τμηματοποιείται σε διαστήματα και η πρώτη δράση ελέγχου ($u_k$) για την τρέχουσα χρονική στιγμή εφαρμόζεται στο σύστημα. Στη συνέχεια ο ελεγκτής μέσω ανατροφοδότησης λαμβάνει υπόψη του την απόκριση του συστήματος που διορθώνει την εκτίμηση του μοντέλου για την νέα εφαρμογή του κριτηρίου βελτιστοποίησης. Η επίλυση του προβλήματος υπολογίζει τη βέλτιστη τιμή των χειραγωγούμενων μεταβλητών ώστε να υπάρξει η επιθυμητή απόκριση της διεργασίας από τις επιβαλλόμενες δράσεις ελέγχου. Η διατύπωση του NMPC αλγόριθμου είναι:

$$\min_{u} J = \sum_{j=1}^{N_p}\left[(\hat{y}_{k+j} - y_{sp,k+j})^T\, Q\left(\hat{y}_{k+j} - y_{sp,k+j}\right)\right] +$$

$$\sum_{i=0}^{Nc-1} \Delta u_{k+l}^T R \Delta u_{k+l} \qquad (1)$$

τ.ω.:

$$\dot{x} = f_d(x,u), \quad y = g(x,u) \qquad (2)$$

$$e_k = \left(y_{pred} - y_{meas}\right)_k, \hat{y}_{k+j} = y_{pred,k+j} + e_k \qquad (3)$$

όπου *u,y,x* είναι οι χειραγωγούμενες, οι ελεγχόμενες μεταβλητές και οι μεταβλητές κατάστασης αντίστοιχα, *Q*, *R* είναι οι πίνακες βαρών και το διάνυσμα αποτελείται από τα επιθυμητά σημεία αναφοράς. Η διαφορά μεταξύ της μετρούμενης μεταβλητής και της εκτιμώμενης τιμής σε χρόνο *k* θεωρούμε ότι διατηρείται σταθερή καθ' όλη τη διάρκεια του ορίζοντα πρόβλεψης που ακολουθεί Επιπλέον η ελαχιστοποίηση υπόκειται σε φυσικούς και λειτουργικούς περιορισμούς των χειραγωγούμενων και των ελεγχόμενων μεταβλητών. Στην παρούσα εργασία υπάρχουν δύο μοντέλα, το ιδανικό (μοντέλο συστήματος), και μία υλοποίηση του συστήματος με ένα μη ιδανικό μοντέλο που περιέχει αβεβαιότητες και θόρυβο (πραγματικό σύστημα). Στόχος του ελεγκτή

είναι να ελέγξει κατάλληλα το μη ιδανικό μοντέλο που αντιπροσωπεύει το πραγματικό σύστημα. Στην παρούσα εργασία το μοντέλο του συστήματος αναφέρεται στα διασυνδεδεμένα μοντέλα των υποσυστημάτων του οχήματος υπό μελέτη.

## 1.4 Διαμόρφωση Προβλήματος Ελέγχου

Ο βελτιστοποιητής προσπαθεί να μειώσει την συνάρτηση κόστους (4), η οποία αποτελείται από δύο όρους. Ο πρώτος αυξάνεται όσο μεγαλώνει η απόκλιση της ροπής από την απαίτηση του χρήστη, οπότε ως αποτέλεσμα ο ελεγκτής με κατάλληλες αλλαγές στις χειραγωγούμενες μεταβλητές φέρνει την ροπή του κινητήρα στην επιθυμητή τιμή. Ο δεύτερος όρος είναι μια σιγμοειδής συνάρτηση η τιμή της οποίας αυξάνεται όταν το επίπεδο φόρτισης της μπαταρίας έχει μεγάλη απόκλιση από το επιθυμητό, αναλογικά με το ρεύμα της μπαταρίας και την φορά αυτού. Ως αποτέλεσμα, το επίπεδο φόρτισης της μπαταρίας τείνει προς μια επιθυμητή τιμή και ισχύς από την μπαταρία καταναλώνεται μόνο όταν υπάρχει περίσσια ή η κ.κ. δεν μπορεί να καλύψει τις απαιτήσεις του χρήστη. Καθώς το επιθυμητό επίπεδο φόρτισης είναι μικρότερο του μέγιστου, διασφαλίζεται η αποθήκευση ενέργειας που θα προκύψει από απότομη επιβράδυνση του οχήματος (αναγεννητική πέδηση).

$$min\ J = \sum_{j=1}^{N_p} \left[ w_1 \left(T_{sp} - T\right)^2 + w_2 \left(1 + \frac{I_b}{|I_b|}\left(1 - e^{-|I_b|}\right) \frac{SOC_d - SOC}{SOC_d - SOC_{min}}\right)\right] \tag{4}$$

$$N_C = \frac{(T_c - T_k)}{\Delta t_c} \tag{5}$$

$$N_p = \frac{(T_p - T_k)}{\Delta t_p} \tag{6}$$

Όπου $J$ το κόστος, $w_{1,2}$ βάρη, $T_{sp}$ ζητούμενη ροπή, $T$ ροπή κινητήρα, $I_b$ ρεύμα μπαταρίας, $SOC$ κατάσταση φόρτισης μπαταρίας και $SOC_d$ επιθυμητό επίπεδο φόρτισης μπαταρίας για χρονική στιγμή $k$ του ορίζοντα πρόβλεψης $T_p$, ενώ με $T_c$ αναπαρίσταται ο ορίζοντας ελέγχου ο οποίος υλοποιείται σε $N_c$ περιόδους δειγματοληψίας.

Επιπλέον, η διαδικασία της ελαχιστοποίησης υπόκειται σε περιορισμούς των χειραγωγούμενων μεταβλητών:

$$I_{fc\,min} \leq I_{fc\,k+j-1} \leq I_{fc\,max} \quad (7)$$

$$I_{b\,min} \leq I_{b\,k+j-1} \leq I_{b\,max} \quad (8)$$

$$V_{air\,min} \leq V_{air\,k+j-1} \leq V_{air\,max} \quad (9)$$

$$V_{fuel\,min} \leq V_{fuel\,k+j-1} \leq V_{fuel\,max} \quad (10)$$

Όπου $I_{fc}$ ρεύμα κ.κ., $W_a$, $W_f$ ροές αέρα και καυσίμου αντίστοιχα. Δύο συναρτήσεις μη γραμμικών περιορισμών (11),(12) καθορίζουν τα επίπεδα των τιμών των λόγων περίσσειας των αντιδρώντων $\lambda_{O2}$,$\lambda_{H2}$ (13),(14) για την προστασία της μεμβράνης της κ.κ. και την επιμήκυνση του χρόνου ζωής. Ο ελεγκτής περιορίζει τις τιμές $C_{1,2}$ στο αρνητικό ημιεπίπεδο, όπου και βρίσκονται όταν οι λόγοι περίσσειας είναι στο επιτρεπτό εύρος λειτουργίας. Ο λόγος περίσσειας για κάθε αντιδρόν εκφράζεται ως ο λόγος της ποσότητας που εισέρχεται στο σύστημα ($W_{H2in}$,$W_{O2in}$) σε σχέση με την ποσότητα που καταναλώνεται από την αντίδραση ($W_{H2react}$, $W_{O2react}$).

$$C_1 = |1.5 - \lambda_{H2}| - 0.2 \quad (11)$$

$$C_2 = |1.9 - \lambda_{O2}| - 0.3 \quad (12)$$

$$\lambda_{H2} = \frac{W_{H2in}}{W_{H2react}} \quad (13)$$

$$\lambda_{O2} = \frac{W_{O2in}}{W_{O2react}} \quad (14)$$

## 1.5 Αξιολόγηση Συμπεριφοράς του Συστήματος

Η προσομοίωση έγινε σε χρονικό πλαίσιο διακοσίων δευτερολέπτων για δεδομένο κύκλο οδήγησης (απαιτήσεις ροπή χρήστη), με αρχική φόρτιση μπαταρίας στο 90%, και επιθυμητή τιμή φόρτισης 95%. Ως κύκλος οδήγησης ορίζεται το σύνολο δεδομένων που αντιπροσωπεύουν τις απαιτήσεις του χρήστη σε μια τυπική διαδρομή. Ο ορίζοντας

πρόβλεψης (χρόνος που υπολογίζεται η μελλοντική συμπεριφορά του συστήματος με την χρήση του ιδανικού μοντέλου) είναι 3 δευτερόλεπτα. Στο Σχ. 1 διακρίνονται οι ισχύς των δύο πηγών (μπαταρία, κ.κ.), του κινητήρα και η ζητούμενη. Είναι εμφανές ότι η μπαταρία αξιοποιείται σε απότομες αυξήσεις του φορτίου, ενώ τον υπόλοιπο χρόνο η ισχύς της είναι αρνητική διότι φορτίζει για να φτάσει το επιθυμητό επίπεδο.

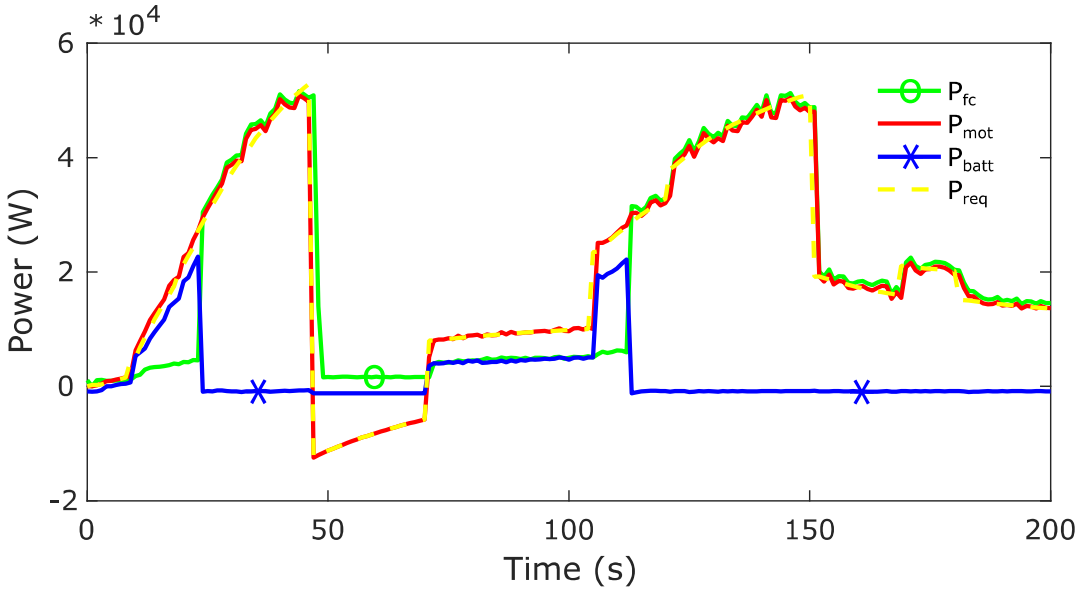

Σχήμα 1: Ισχύς κ.κ., κινητήρα, μπαταρίας, ζητούμενη

Στο Σχ. 2 φαίνεται ο κύκλος οδήγησης υπό την μορφή απαιτούμενης από τον χρήστη ροπής, και η ροπή που παράγει ο κινητήρας ως αποτέλεσμα των δράσεων του ελεγκτή.

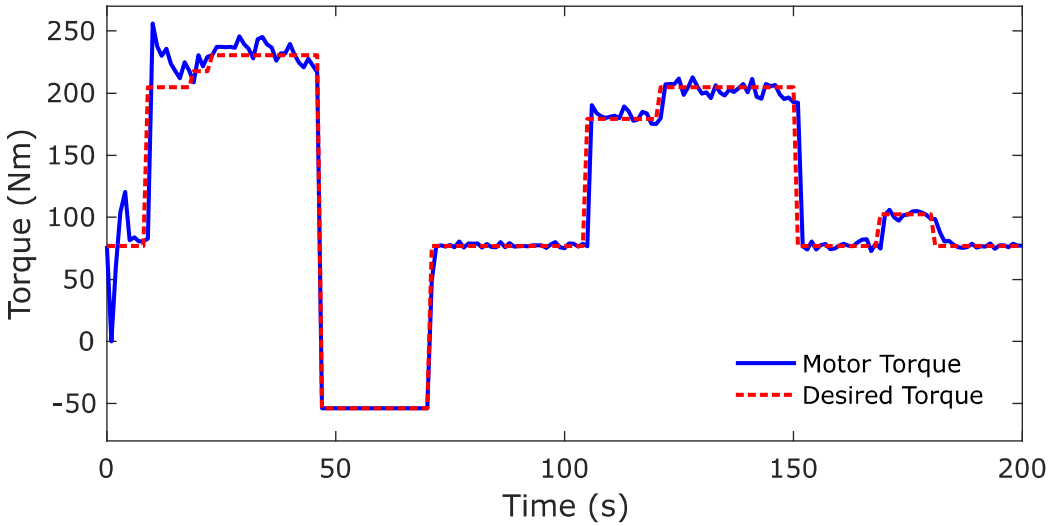

Σχήμα 2: Ροπή κινητήρα, ζητούμενη ροπή

Στο Σχ. 3 διακρίνεται το επίπεδο φόρτισης της μπαταρίας, το οποίο μειώνεται στις περιόδους χρήσης της και τον υπόλοιπο χρόνο φορτίζει από την κυψέλη καυσίμου.

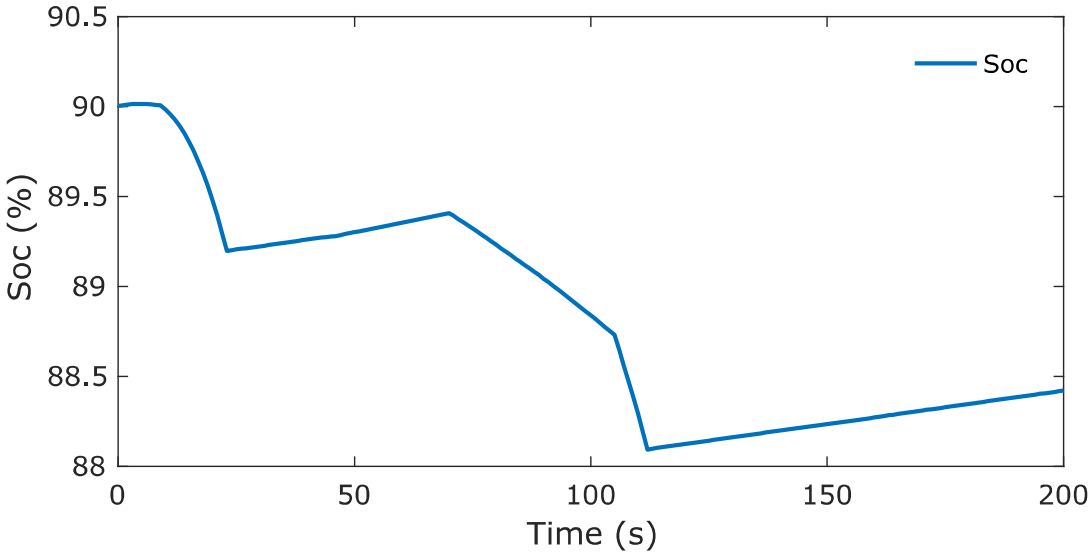


Σχήμα 3: Επίπεδο φόρτισης μπαταρίας

Η επίδραση των περιορισμών φαίνεται στο Σχ. 4, όπου οι τιμές των λόγων περίσσειας των αντιδρώντων μένουν στα επιθυμητά πλαίσια (διακεκομμένες γραμμές).

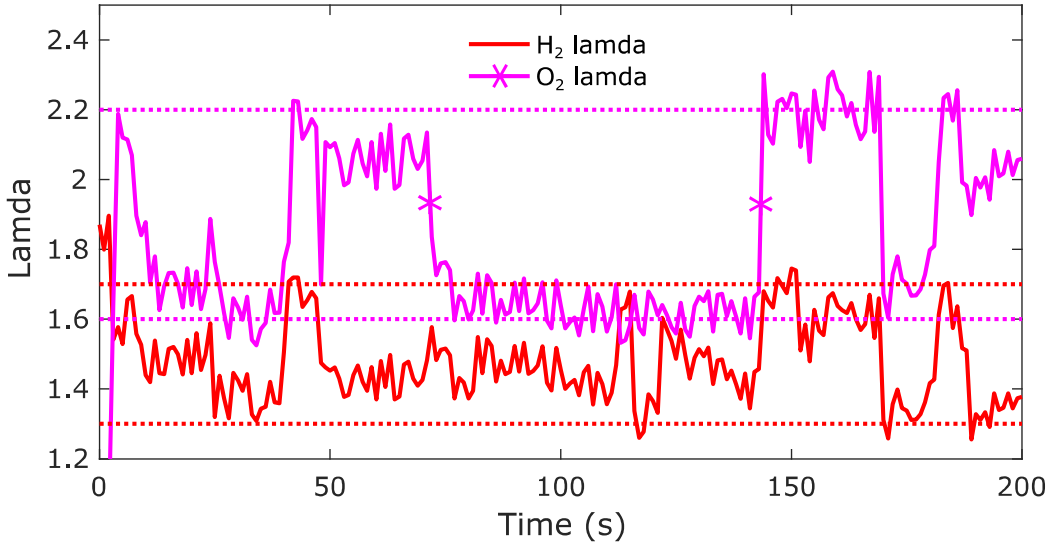


Σχήμα 4: Λόγος περίσσειας υδρογόνου, οξυγόνου

Στο Σχ. 5 υπάρχουν οι χειραγωγούμενες μεταβλητές (έξοδος του ελεγκτή): ροή καυσίμου σε λίτρα ανά λεπτό, ροή αέρα, ρεύμα μπαταρίας σε ampere, ρεύμα κυψέλης καυσίμου. Αυτές είναι οι τιμές που εφαρμόζονται στο μοντέλο του «πραγματικού» συστήματος.

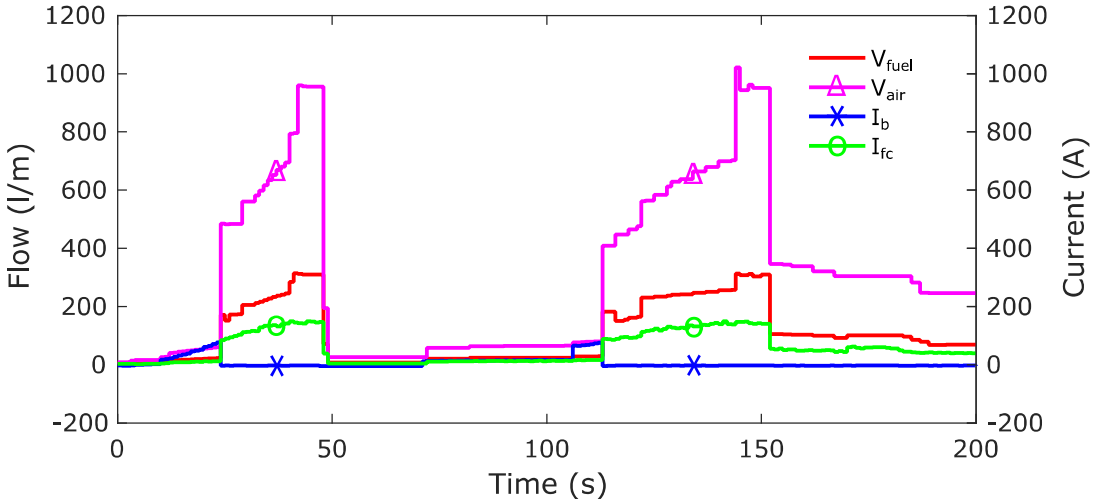

Σχήμα 5: Ροή υδρογόνου, αέρα (λίτρα/λεπτό), ρεύμα μπαταρίας, κ.κ.

Είναι εμφανές από τα αποτελέσματα ότι ο ελεγκτής που υλοποιήθηκε καλύπτει τις απαιτήσεις του χρήστη αλλά ταυτόχρονα επιτυγχάνει ικανοποιητική διαχείριση ενέργειας μεταξύ τον δύο πηγών, αλλά και λαμβάνει υπόψιν την σωστή λειτουργία της κυψέλης καυσίμου.

## 1.6 Συμπεράσματα

Στην παρούσα εργασία αναπτύχθηκε ένα δυναμικό μη γραμμικό μοντέλο του οχήματος με τα υποσυστήματα αυτού, και υλοποιήθηκε ένας προρρητικός ελεγκτής NMPC που ικανοποιεί τους λειτουργικούς περιορισμούς του συστήματος. Συμπεριλαμβάνοντας όλους τους στόχους ελέγχου στον ίδιο ελεγκτή, διασφαλίζεται η σωστή λειτουργία ολόκληρου του συστήματος και όχι μόνο των επιμέρους στοιχείων που το αποτελούν, διότι μπορεί μονομερώς αποδεκτές λύσεις να μην είναι συμβατές στο σύνολό τους. Το γεγονός ότι χρησιμοποιείται το μη γραμμικό μοντέλο του συστήματος εξασφαλίζει την πρέπουσα συμπεριφορά του ελεγκτή σε ένα μεγάλο εύρος και όχι μόνον σε μια γραμμική περιοχή λειτουργίας. Διαπιστώθηκε ότι η προτεινόμενη προσέγγιση είναι δυνατόν να εφαρμοστεί σε πολυμεταβλητά μη γραμμικά προβλήματα ελέγχου.

# 2

# Introduction

The purpose of this chapter is to introduce the reader to the technology of fuel cells, their applications and advantages, as well as to the use of hydrogen as an energy carrier and hybrid vehicles. The importance of control is also highlighted as it is a vital branch of engineering in the advancement of technology.

## 2.1 The environment and the future of transportation

As the concerns over climate change increase, alternative environmentally friendly transport systems and renewable energy systems are becoming more attractive. It is widely known that the energy demand worldwide is increasing. In order to meet the increased demand, reserves of fossil fuels such as oil are used, which are gradually diminishing. On the other hand the use of fossil fuels is a source of greenhouse gasses and other pollutants that cause global warming with very serious and irreversible effects on the environment. For example between 1990 and 2010 90 % of the increase in $CO_2$ is attributed to the transport sector. More specifically road transport is responsible for 85% of the $CO_2$ emissions. The fact that an average lorry generates six times more $CO_2$ per ton/km than a train raises significant questions regarding the required actions that will firstly reduce this effect and secondly will decarbonize the road transport and the energy sector.

In that context, electric vehicles (EVs) and fuel cell EVs aim to be part of the future transport sector. The shift towards a low carbon, efficient and secure economy requires targeted deployment of innovative technologies and increased exploitation of renewable energy sources. [6] Furthermore, it is recognized that a technological shift and the development of new clean technologies are vital for a successful transition to a decarbonized and sustainable future economy. Although a number of diverse technologies exist that aim at the same target, such as biofuels and carbon capture and storage, the synergy between the increased use of renewable energy sources, renewable hydrogen and electricity from fuel cells represent one of the promising ways to realize sustainable energy. These technologies can simultaneously address the environmental concerns and the issues of security in energy supply and are considered as key solutions for the 21st century. Hydrogen and fuel cells can enable the so-called hydrogen economy and they can be utilized in transportation, distributed power and heat generation and energy storage systems.

## 2.2 Hydrogen as an energy source

The endeavor of achieving a low carbon economy can be greatly facilitated by the use of hydrogen which is not a primary energy source like coal and gas but it is an energy carrier with zero carbon content. Hydrogen is a very attractive fuel that can be obtained by a variety of diverse resources which means that it can alleviate the issue of energy security which is related to the confined production of a fuel at specific regions on the planet. Since hydrogen can be produced anywhere where there is water and a source of power, generation of fuel can be distributed and does not have to be grid-dependent. Thus the long-term use of hydrogen can decouple the link between the energy needs and the energy supply. It can be produced from all primary energy sources and generates no $CO_2$ when used to generate electricity in a fuel cell system or alternatively it can be produced from fossil fuels with $CO_2$ capture and storage technologies. Furthermore, it can be used in a number of applications ranging from devices and products powered by fuel cells to heat and power generators in stationary systems for industrial and domestic use. Thus, the use of hydrogen could drastically reduce GHG emissions from the energy sector.

Hydrogen as an energy carrier can create links between a multitude of production methods and sources to various applications including fuel cell systems. But its usefulness is not limited to those. It offers an interesting solution for both short and long-term storage in small or bulk quantities. In cases where the supply is more than the demand, the excess of energy can be transformed into hydrogen that can be easily transported or remain onsite and serve the needs for power on demand. The transportation of hydrogen can be achieved by a number of alternatives including vehicle, ships and pipelines. Thus, the most cost-efficient method can be selected per case. Also, it can facilitate the integration of renewables in the energy supply system and offer the opportunity to increase the share of renewable energy. In the case of intermittent sources hydrogen can act as a temporary energy storage option that utilizes the excess of energy supply subsequently used to balance the demand upon request.

Overall hydrogen is expected to play an important role in the future low carbon energy landscape and it can be used to close the cycle of energy generation, distribution and demand. However, the transition from a carbon-based energy economy to a hydrogen-based one involves significant scientific and technological challenges for the implementation of hydrogen in conjunction with fuel cells as a clean energy solution of the future.

## 2.1 Fuel cells

Fuel cells are electrochemical devices that directly convert chemical energy stored in the fuel (in this case H2) to electricity producing water and heat. Since there are no mechanical parts, they are very reliable (assuming the right operational conditions) and have a silent operation, a feature that together with the zero greenhouse emissions makes them very attractive for automotive use. Assuming that the hydrogen to be consumed by the vehicle is produced from renewable sources, the carbon footprint of this mean of transportation is minimal.

Humphry Davy effectively demonstrated the concept of a fuel cell in the early nineteenth century. Pioneering work followed by Christian Friedrich Schönbein in 1838 on what would become fuel cells are they are known today. The invention of fuel cells is generally credited to William Grove for his series of experiments conducted in 1839

in what he termed “gas voltaic battery” which proved that electric current could be produced from an electrochemical reaction between hydrogen and oxygen with the presence of a catalyst. The term fuel cell was first used in 1889 by Charles Langer and Ludwig Mond, who researched coal gas fuel cells. The first practical system demonstrated was an alkaline fuel cell developed by Francis Thomas Bacon.

Between 1950 and 1960, NASA worked in collaboration with other industrial partners in order to develop fuel cells to be used in manned space missions. As a result, the first proton exchange membrane fuel cell was constructed with its invention credited to Willard Thomas Grubb, and later refined by Leonard Niedrach to be used in the Gemini space program.

Increasing environmental awareness in the 1970s prompted concerns over air pollution which eventually led to clean air legislation in the United States and Europe, mandating the reduction of harmful vehicle exhaust emissions. Together with the fact of zero emissions operation of fuel cells, this increased the attractiveness of FC technology for vehicular applications and several manufacturers followed the initiative of General Motors which was already experimenting with a fuel cell car, the 1966 *Electrovan*.

A more recent concept FCEV was introduced in 2008, the Honda *FCX Clarity*. The lack of hydrogen infrastructure though did not allow broad adoption and as such it was only available for lease. It would not be until 2015 that a fuel cell electric vehicle would be commercially produced with the Toyota *Mirai* (Japanese for "future"), with about 3000 unit sales worldwide with Japan being the top selling market closely followed by the United States. Subsequent production models include the Honda *Clarity* and Hyundai *Tucson FCEV*, both only available on leasing agreements.

A more widespread use of fuel cells in vehicles can be seen in forklifts, and experimental deployment is being trialed in buses, boats, trains and even airplanes.

The power output of the FC depends on the partial pressures of the fuel and oxidizer in the anode and cathode respectively, which in turn depend on the air compressor and manifold filling dynamics, and as a result there is a time delay induced in sudden power demand variations. Furthermore, such abrupt variations drive the fuel and air excess ratios (lambda) in undesired values that hasten the degradation of the membrane of the

FC and can even lead to its destruction. The need for a supplementary power source with faster dynamics arises, which can provide the needed electric current to satisfy the demand on abrupt changes without unnecessary stress on the FC. This need is often satisfied with the addition of a battery, which can provide power during fast transients and has the added benefit of being able to store excess energy recovered from the motor while decelerating (regenerative braking). With this addition the complexity of the system is increased and the problem of power management between the two sources is introduced. Because of the presence of two power sources, the vehicle can now be classified as a hybrid.

## 2.2 Hybrid electric vehicles

The first design attempts for a hybrid electric vehicle can be traced as early as 1889, with a gasoline-electric hybrid rail car patent application filed by William H. Patton. A generator driven by a gasoline engine charged a battery connected in parallel to the driving motors, making the vehicle a series hybrid. A subsequent prototype named *Armstrong Phaeton* was developed by Harry E. Dey in 1896 which was significantly innovative, featuring a gasoline internal combustion engine whose flywheel was connected to a motor capable of charging its battery, starting the engine, providing additional power alongside the engine or even harvesting part of the otherwise lost energy during braking. Other examples of primitive series hybrid electric vehicles include the *Mixte* developed in 1900 by Ferdinand Porsche or the *Dual power* hybrid (1915) produced by *Woods Motor Vehicle*.

Development of hybrid electric vehicles continued throughout the 20$^{th}$ century with the notable work of Victor Wouk, Audi and Volvo experimental vehicles which would become the predecessors to modern hybrids.

In 1997, Toyota launched *Prius*, the first mass produced hybrid vehicle, capable of operating either only with the combustion engine or the electric motor, or even with both at the same time, classifying it as a series – parallel (full) hybrid. The first commercial success of a hybrid vehicle marked the start of an era. Other manufacturers followed, most notably Honda with *Civic hybrid*, Ford with the *Escape hybrid* and Lexus with *GS 450h*. Since then, a multitude of manufacturers offer hybrid vehicles as

a response to the increasing demand, with more than 12 million sold since their 1997 appearance.

## 2.3 The importance of control

Systems and process control is an important area both from scientific and technological point of view, able to facilitate the improvement of the response and overall behavior of systems, processes and end-user applications. Thus, it is important for the control technologies to be built upon a rigorous sensing, modeling, decision making and optimization basis as in many situations, the subsystems of a process have high degrees of autonomy and heterogeneity. Therefore, a continuous research effort is imperative for the realization of system-level goals for performance, predictability, stability, and other properties through appropriate analysis, design and implementation. In this context, the proper control structure and methods can function as a catalyst that transforms technological innovation to systems engineering and process novelties. At a wider context, control engineering tools and platforms are used to facilitate the analysis and modeling of the system and explore its response and behavior. Besides that, control is necessary to overcome the limits of ad hoc solutions as it is a highly scalable technology. Nowadays, control is present at various levels of a system or a process, initially it is applied to individual sensors and actuators, then on multivariable systems, and finally at plant wide scale. The impact of control technology is evident in a wide range of application areas, including fuel cells, as it is the necessary facilitator for achieving desired objectives and fulfilling application-specific goals. Fuel cell systems exhibit fast dynamics, nonlinearities and uncertainties that constitute challenges requiring appropriate control in order to be confronted effectively. The use of efficient control strategies would not only increase the performance of these systems, but would increase the number of operational hours as their lifetime is preserved by operating at optimal levels and also reduce the cost per produced kilowatt-hour. Overall control can be considered as a key enabling technology for the deployment of fuel cell systems as well as renewable energy systems.

The importance of expanding the use of clean hydrogen energy in the transportation sector makes studying the control of fuel cell applications in vehicles worthwhile.

# 3

# Literature Review

For accurate simulation, it is imperative that the mathematical models used have a high degree of precision. Reproducing the characteristics of a fuel cell as a function of the load current is not a simple task and multiple approaches are present in literature, such as dynamic models of a PEM FC derived from material and energy balances as well as electrochemical and semi-empirical equations [7] or models that foresee the FC stack performance in situations commonly encountered in electrical power generation systems, like insertion and rejection of loads, efficiency, and power characteristics, which also incorporate the essential physical and electrochemical processes that happen in the cell during its operation. [8] Other implementations along with the physical principles of the system include stack polarization data, dynamics of the air compressor, manifold filling dynamics and time-evolving reactant mass, aiming at a model more suitable for control oriented studies. [9]

For such applications and specifically model predictive control implementations, for the design and simulation of the system a simple but realistic and accurate model is desired that can reproduce the characteristics of the FC system with minimal computation time and tuning parameters so that the development of several control techniques will be possible.

A generic FC model able to represent the behavior of most FCs fed with hydrogen and air that requires only a few variables from the manufacturer's datasheet is presented in [4]. Apart from the immediate advantages a non-linear model has regarding the

accuracy, the ability to extract the parameters needed for the formulation of the model from the datasheet without the demand of experimental tests for each FC stack is favorable because of the ease of application it provides on real systems. This particular model offers acceptable performance both in behavior and execution time, a crucial factor when it is to be used in an MPC control scheme.

Formulating an exact battery model is a complex endeavor that requires extensive electrochemistry knowledge, although the use of such an involved model in not necessary for transport related applications. It is more important that the model provides the general behavior of a battery regarding the state variables of interest, such as the deviation of the open-circuit voltage according to the state of charge. Equivalent electric circuit models provide sufficient accuracy in representing the electrical characteristics and behavior of batteries, and experimental validation concludes that there is an adequate representation of the behavior of a real battery. [10] A less involved version of this model is presented in [3], which also has the benefit of easy parameter extraction from the datasheet of the battery. Using the state of charge of the battery as a state variable of a controlled voltage source in series with a resistance, there is an accurate representation of four different battery types.

There has been a multitude of propositions for the energy management of fuel cell hybrid vehicles, with approaches ranging from low level current control using frequency management techniques to adaptive MPC controllers. Frequency energy management is based on satisfying energy and power constraints of each source given its specific power/energy capability. It ensures compatibility between the frequency components of the mission and the intrinsic frequency capacities of the different sources [11]. Other examples include voltage control loop energy management [12], and PI controllers [13][14]. In a voltage control loop setup, the fuel cell charges the battery and the battery in turn charges the supercapacitor to which the load is connected, using voltage setpoints. The energy management strategy based on dynamic classification aims at distributing the required power of the vehicle among the sources in a way that each source is used optimally. PI energy management implementations include controlling the State of Charge of the battery together with FC efficiency terms, or current control derived from a heuristic energy management algorithm.

Although the aforementioned methods are suitable for applications with uninvolved requirements, when multiple operational targets are present then there is a growing need for more sophisticated or complex techniques that are deployed for the optimum control of the hybrid FC powertrain for vehicular applications.

Examples of innovative implementations include fuzzy logic controllers [15] and optimal solutions with Markov chain prediction capabilities [16]. Fuzzy logic control is a non-linear control method that gives robust performance without the need of a mathematical model of the plant. The basis is straight forward and is expressed in natural language. Fuzzy logic is adaptable and can deal with imprecise data. The incorporation of Markov chains in optimal control is an attempt to predict future conditions in order to improve the performance of the controller. A Markov chain is a stochastic process that satisfies the Markov property, i.e. can make predictions for the future of the process based solely on its present state, without the information of the process' history.

Besides the aforementioned methods, the use of optimization-based techniques are employed for the multi-variable nonlinear energy management problem of the FCEV. The optimal operation of such systems has been studied [17] and is a very promising solution to the presented problems. Adaptive optimization techniques [18][19] have also been suggested that take into account the variations in the performance of the FC due to degradation over time or different operating conditions. An adaptive optimal control energy management system (AOC-EMS) is able to fabricate an optimal EMS using reinforcement learning. In case a neural network is utilized, a pretraining procedure is required to obtain convergent weights.

To apply such optimal control solutions to a physical system in real time, Model Predictive Controllers are utilized, which apart from guiding the system to an optimal operating point under various conditions, also take in account multiple constraints and control objectives. Existing MPC implementations have been studied such as ref. [2] with a linear model implementation of a similar system and a hybrid predictive controller in conjunction with a piecewise affinity model (explicit MPC). The main argument for explicit formulation is to reduce the computational time by performing the optimization when the controller is off-line and search for the solution when on-

line. The use of an MPC controller for the energy management [1],[20] has been validated experimentally [21] and is proven to be effective in practice.

A significant advantage of MPC controllers is the ability to integrate multiple control objectives by manipulating various aspects of the system in order to reach a universal solution.

# 4

# System Description

This chapter deals with the characteristics of the specific system under study, its topology and specifications of the subsystems.

## 4.1 System Topology

In order to study the behavior of the FCEV, the mathematical model of the system is developed. Each subsystem is individually modelled and tested using data available in the literature in order to verify that the behavior is characteristic of the specific component.

Figure 1 shows the three subsystems: the fuel cell, the electrical and the motor subsystem. The supervisory controller is responsible for the power split between the two power sources and the fuel – oxidizer input flow rates of the FC. The main energy provider is the fuel cell and the secondary is the battery.

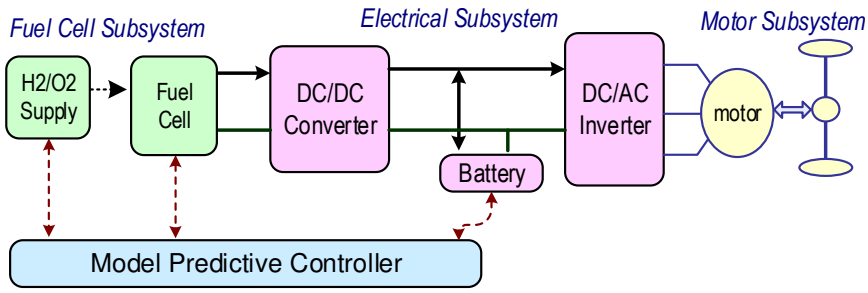


Figure 1: System overview

More specifically the FCEV is comprised of the following components: a Polymer Electrolyte Membrane (PEM) fuel cell stack which acts as the main source of power; a Lithium-ion Battery – the secondary power source; a Permanent Magnet Synchronous Motor (PMSM) which is tasked with the conversion of the stored energy in order to achieve propulsion and the power electronics (DC/DC converter and 3-phase DC/AC inverter) required in order to couple the various components. The specifications of the subsystems can be seen in Table 1.

TABLE 1: SUBSYSTEM DETAILS

| Component | Specifications |
|---|---|
| PEMFC | Power: 85 kW (nominal), 100 kW (maximum)<br>Voltage: 288 Vdc (nominal)<br>Efficiency: 58 % (average)<br>Temperature: 75 °C<br>Pressure: 3 bar<br>Fuel consumption: 374 l/m (nom.)<br>Air consumption: 1698 l/m (nom.) |
| Li-Ion Battery | Power: 25 kW<br>Capacity: 20 Ah<br>Voltage: 288 Vdc |
| PSM Motor | Power: 100 kW<br>Torque: 256 Nm |
| DC/DC converter | Efficiency: 95 % |

Table 2 shows the variable classification for the complete FCEV system.

TABLE 2: FCEV VARIABLES

| Input Variables | State Variables | Output Variables |
|---|---|---|
| FC current | Battery SOC | Vehicle speed |
| Battery current | | Motor torque |
| FC Fuel flow | | FC fuel excess ratio |
| FC Air flow | | FC air excess ratio |

## 4.2 Proton Exchange Membrane Fuel Cell

A semi-empirical model for the fuel cell is used [4]. Table 3 presents the input and output variables of the fuel cell model.

TABLE 3: FUEL CELL MODEL SPECIFICATIONS

| Inputs | Outputs |
|---|---|
| Air flow rate/pressure | Excess $H_2$ (lambda) |
| Fuel flow rate/pressure | Excess $O_2$ (lambda) |
| Percentage of H2 in the fuel mix | Voltage |
| Percentage of O2 in the air mix | |
| Operation Temperature | |
| Stack Current | |

At first the rates of conversion (utilization) are calculated for the anode (15) and the cathode (16), which are in turn used to calculate the partial pressures of the reacting gasses (19),(20). Then the Nernst voltage is computed (21) and the voltage constant at the nominal condition (22), in order to derive the open circuit voltage (23) and the controlled voltage source voltage (24). Finally the final FC voltage is a function of the controlled voltage source, the internal resistance of the FC and the stack current (25).

$$U_{fH2} = \frac{60000RTNi_{fc}}{zFP_{fuel}V_{fuel}x_{\%}} \quad (15)$$

$$U_{fO2} = \frac{60000RTNi_{fc}}{2zFP_{air}V_{air}y_{\%}} \quad (16)$$

$$\lambda_{H2} = \frac{W_{H2in}}{W_{H2react}} \quad (17)$$

$$\lambda_{O2} = \frac{W_{O2in}}{W_{O2react}} \quad (18)$$

$$P_{H2} = \left(1 - U_{fH2}\right)x_{\%}P_{fuel} \quad (19)$$

$$P_{O2} = \left(1 - U_{fO2}\right) y_{\%} P_{air} \tag{20}$$

$$E_n = 1.229 + (T - 298)\frac{-44.43}{zF} + \frac{RT}{zF} ln\left(P_{H2} {P_{O2}}^{\frac{1}{2}}\right) \tag{21}$$

$$K_c = \frac{E_{ocnom}}{E_{nnom}} \tag{22}$$

$$E_{oc} = K_c E_n \tag{23}$$

$$E = E_{oc} - NAln\left(\frac{i_{fc}}{i_0}\right) \tag{24}$$

$$V_{fc} = E - R_{ohm} i_{fc} \tag{25}$$

Where

$U_{fx}$: utilizations, $R$: gas constant (J mol$^{-1}$ K$^{-1}$), $z$: number of moving electrons, $F$: Faraday constant (A s mol$^{-1}$), $P_x$: partial pressures (atm), $V_x$: flow rates (l/min), $x\%$: percentage of hydrogen in the fuel, $y\%$: percentage of oxygen in the air, $\lambda_x$: excess ratios, $W_{xin}$: entering mass flow rate, $W_{xreact}$: rate of reacted mass, $T$: operation temperature (K), $K_c$: voltage constant at nominal operation, $E_{ocnom}$: nominal open circuit voltage (V), $E_{nnom}$: nominal Nernst voltage (V), $E_{oc}$: open circuit voltage (V), $E$: controller voltage source voltage (V), $N$: number of cells, $A$: Tafel slope (V), $i_{fc}$: fuel cell current (A), $i_0$: exchange current (A), $V_{fc}$: fuel cell voltage (V), $R_{ohm}$: internal resistance (Ω)

The calculation of the intermediate state variables required by the fuel cell model is separated in three virtual blocks of operations, as depicted in Figure 2. After the final output values from the blocks have been computed, the emulation of the fuel cell electrical circuit takes place and all the model outputs are then available for further use.

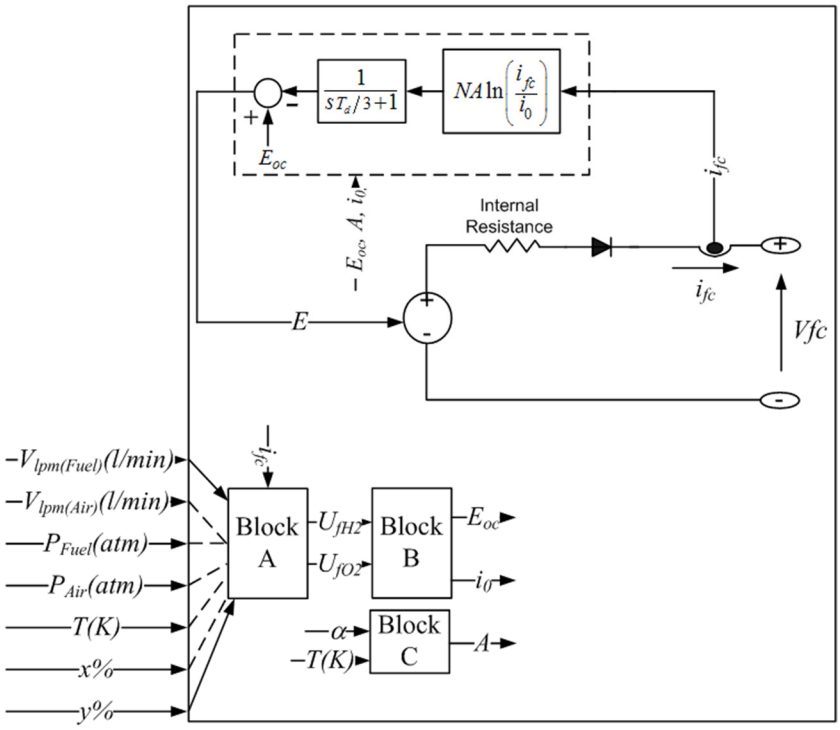


Figure 2: Detailed fuel cell stack model

The FC model response was validated in comparison to the literature model, as presented in Figure 3.

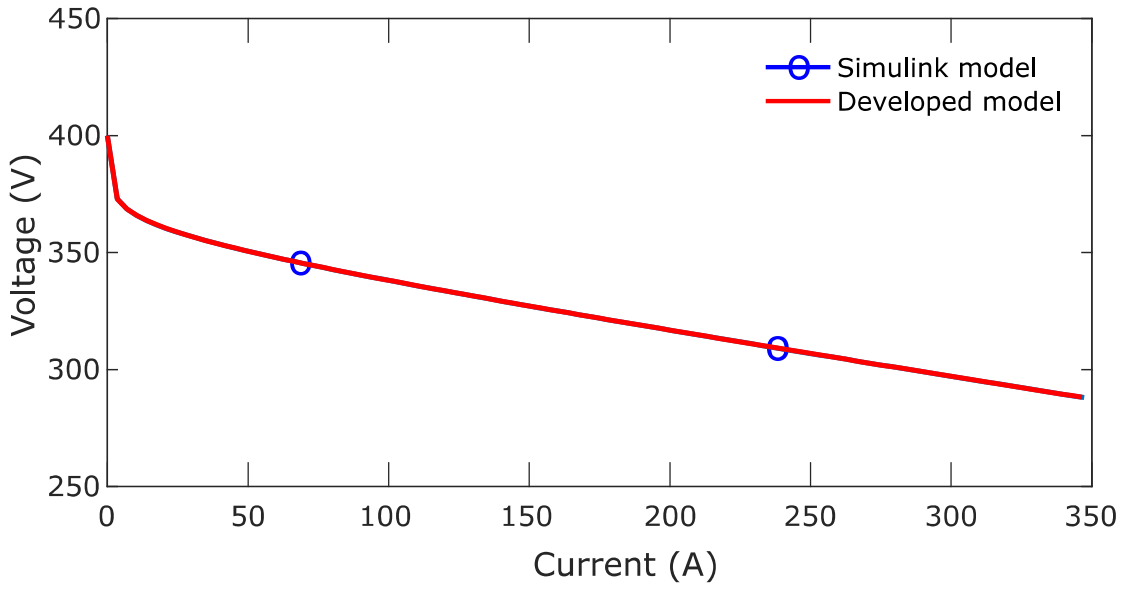


Figure 3: FC models I-V curve comparison

In Figure 4 the value of two outputs of the fuel cell model (stack voltage and hydrogen excess ratio) is shown in respect to three of the inputs (stack current, fuel flow rate and oxidizer flow rate).

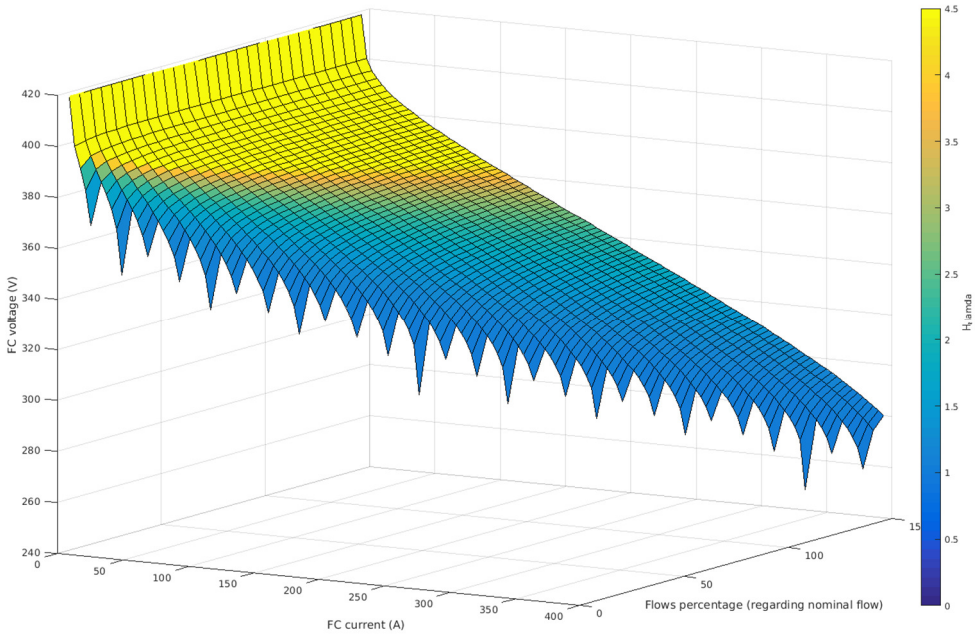


Figure 4: Stack voltage and hydrogen excess ratio

## 4.3 Li-Ion Battery

The battery model [3] consists of a voltage source $V_{src}$ in series with an internal resistance $R_i$. The battery current $I_b$ is the input of the model, and the voltage $V_b$ is the output. The state of charge is a state variable. Model equations:

$$V_{src} = V_0 - K\frac{Q}{Q-\int_0^t I_b dt} + Aexp\left(-B\int_0^t I_b dt\right) \quad (26)$$

$$V_b = V_{src} - R_i I_b \quad (27)$$

$$Soc = 100\left(1 - \frac{\int_0^t I_b dt}{Q}\right) \quad (28)$$

$$K = \frac{\left(V_{full} - V_{nom} + A(exp(-BQ_{nom}) - 1)\right)(Q - Q_{nom})}{Q_{nom}} \quad (29)$$

Where

$V_{full}$: fully charged voltage (V), $V_{nom}$: nominal voltage (V), $V_0$: battery constant voltage (V), $K$: polarization constant (V $Ah^{-1}$), $A$: voltage drop at the exponential zone (V), $B$: charge at the end of the exp. zone ($Ah^{-1}$), $Q_{nom}$: nominal capacity (Ah) and $Q$: maximum capacity (Ah).

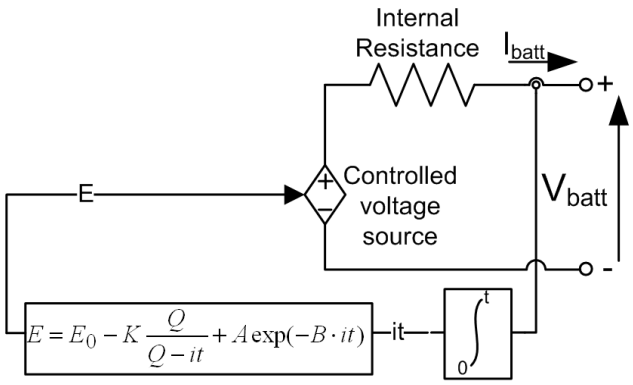


Figure 5: Non-Linear battery model

To verify the validity of the battery model, its response was compared to typical operation of this subsystem according to the literature model [10] with a nominal discharge current of 6.04 A. The depicted deviation in Figure 6 becomes significant only outside the nominal operation zone and is thus irrelevant for the application.

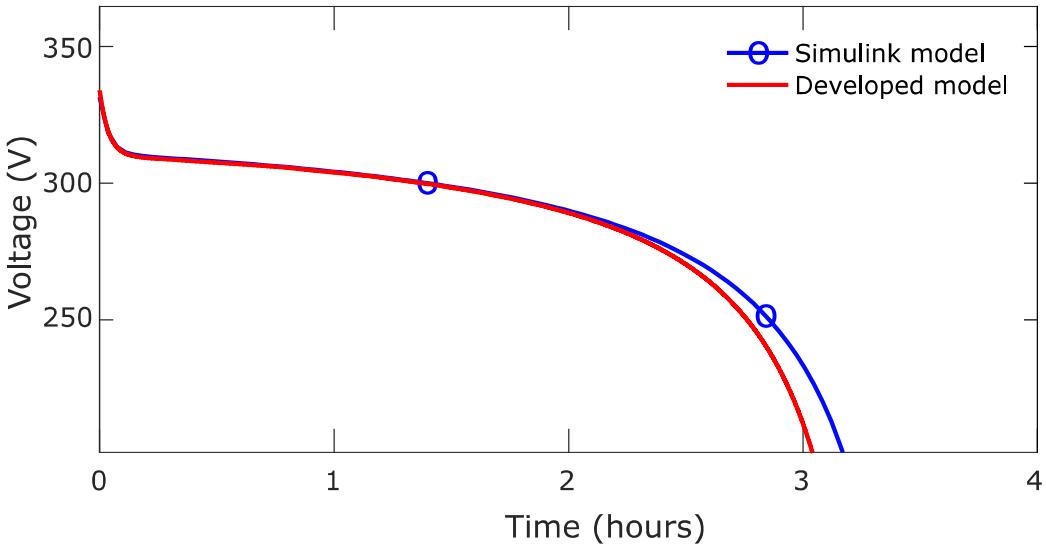


Figure 6: Battery models nominal discharge curve comparison

## 4.4 Vehicle

The vehicle is modeled as a single point with three acting forces, the driving force coming from the motor, aerodynamic drag and friction losses. Using Newton's second law, we can compute the acceleration and thus the speed and position of the vehicle on one dimension. The input is the torque at the motor shaft and the outputs are the motor shaft angular velocity, the vehicle speed, acceleration and the traveled distance.

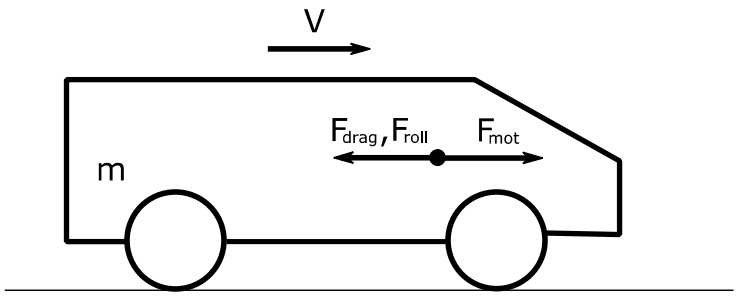


Figure 7: Vehicle model diagram

$$V = \int a\, dt \tag{30}$$

$$a = \frac{F_{mot} - F_{drag} - F_{roll}}{m} \tag{31}$$

$$F_{mot} = \frac{\tau n}{r} \tag{32}$$

$$F_{drag} = 0.5 \rho A_v C_d V^2 \tag{33}$$

$$F_{roll} = (C_0 + C_1|V| + C_2 V^2) mg \tag{34}$$

Where

$m$: vehicle mass (kg), $\tau$: motor torque (Nm), $r$: wheel radius (m), $n$: gear ratio, $\rho$: air density (kg $m^{-3}$), $g$: gravity acceleration (m $s^{-2}$), $A_v$: vehicle frontal area ($m^2$), $C_n$: coefficients, $F_{mot}$: force induced by the electric motor (N), $F_{drag}$: force of the aerodynamic drag (N), $F_{roll}$: rolling resistance force (N).

## 4.5 Sensitivity Analysis

In order to assess the validity of the FCEV model a sensitivity analysis was performed with regard to fuel cell power limitation. The presence of a controller capable of matching the motor torque with the desired torque was assumed, and the current requirement of the motor is fulfilled with the fuel cell as the primary source, utilizing the battery only when the fuel cell cannot meet the demand. Four different fuel cell power limit scenarios were simulated: No limit, 60kW, 30kW, 10kW.

The effect of the power limiting can be seen on the power sources currents and the battery state of charge.

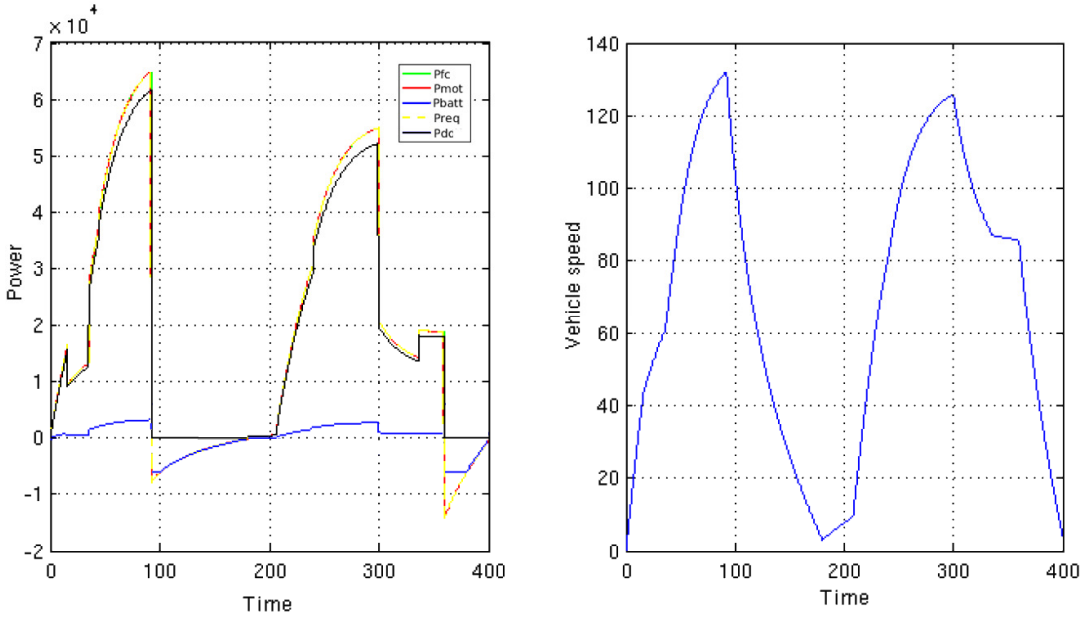


Figure 8: Sensitivity analysis - No fuel cell power limit (1)

In Figure 8a the lack of limit in the fuel cell power availability is evident, as nearly all of the requested power (without accounting the electrical losses) is being drawn from the fuel cell. The speed of the vehicle varies in a smooth way, directly related to the provided torque.

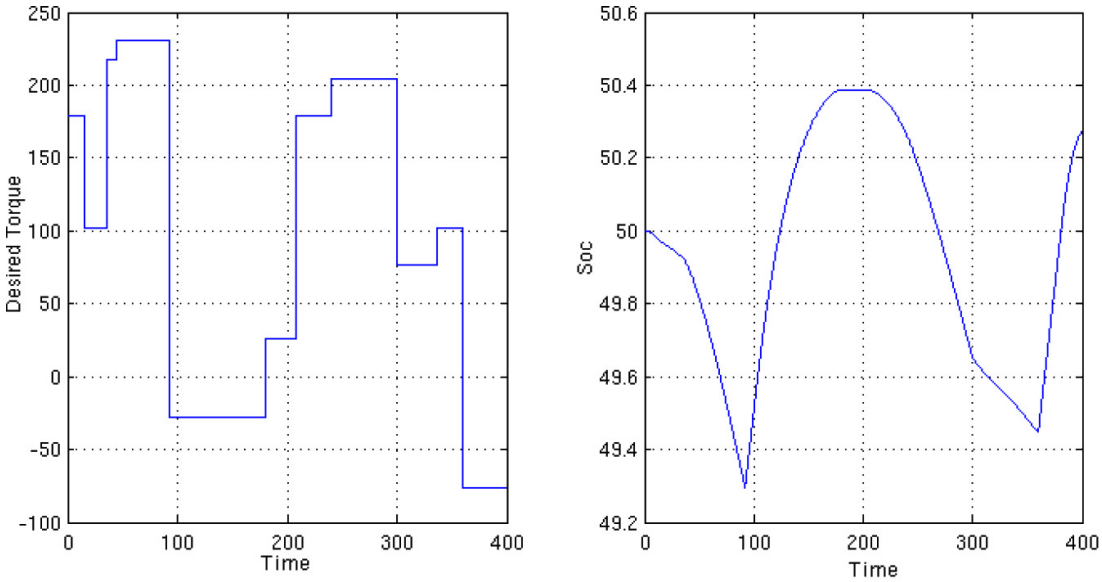


Figure 9: Sensitivity analysis - No fuel cell power limit (2)

In Figure 9a the desired torque is depicted, which correlates to the motor torque due to the absence of a controller. In 9b the state of charge of the battery can be seen decreasing when the battery power is positive, and increasing when it is negative (during braking).

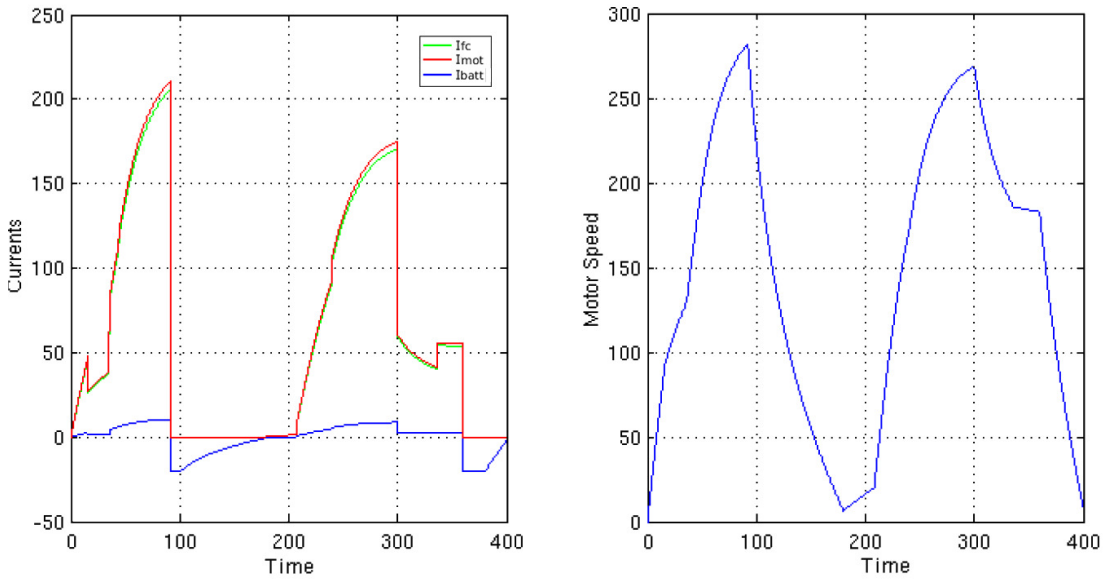


Figure 10: Sensitivity analysis - No fuel cell power limit (3)

Figure 10a presents the currents of the fuel cell, motor and battery and 10b the speed of the motor, to which the vehicle speed is directly related.

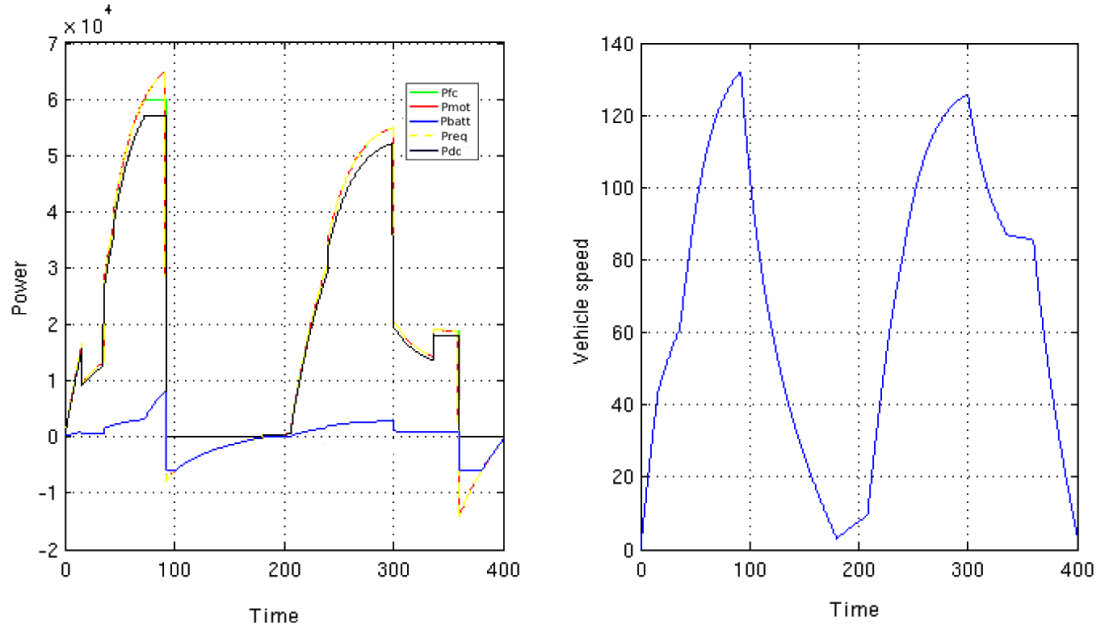


Figure 11: Sensitivity analysis – 60 kW fuel cell power limit (1)

In Figure 11a the upper power limit is now evident, as the fuel cell stops providing power above 60kW and the battery takes over in order to cover the demand.

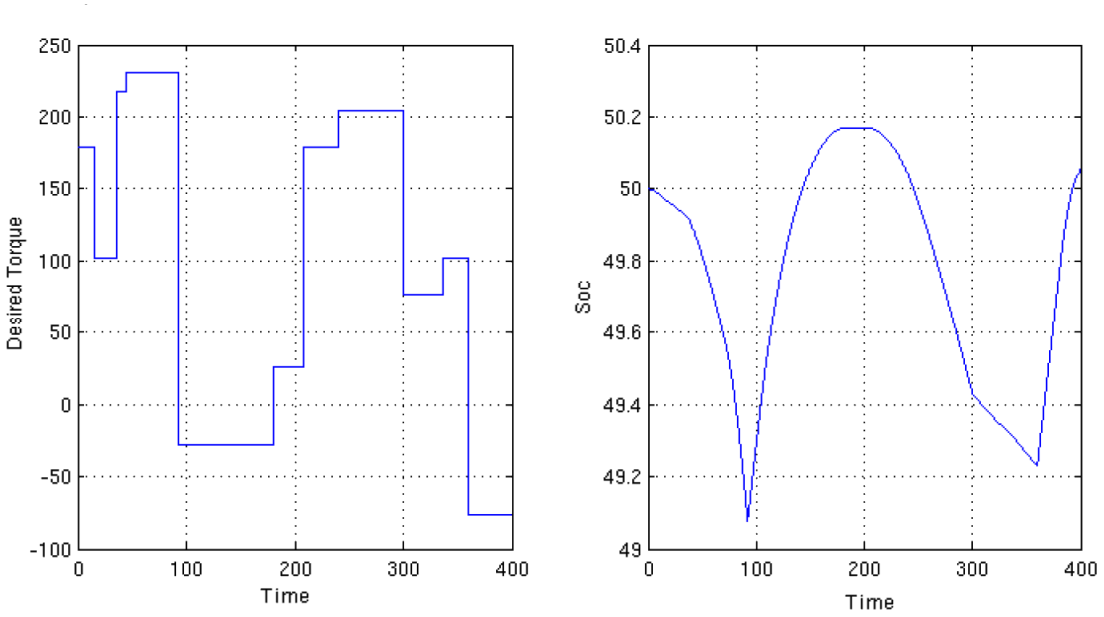


Figure 12: Sensitivity analysis – 60 kW fuel cell power limit (2)

Figure 12a depicts the same driving cycle, and in 12b the effect of the power limiting can be seen as a decrease in the minimum value of the state of charge, as a direct result of the increased battery utilization.

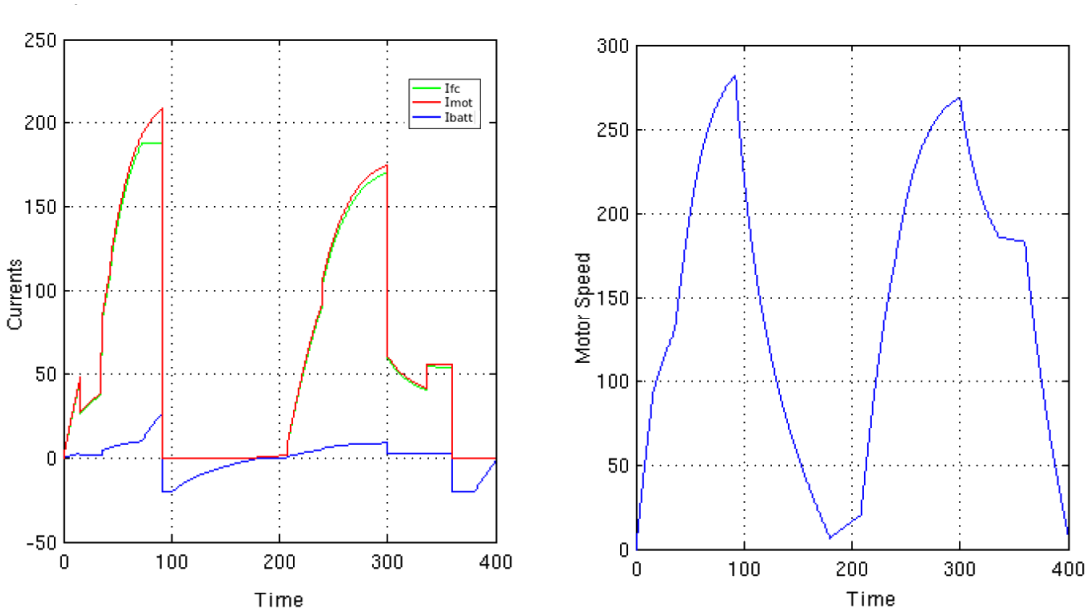


Figure 13: Sensitivity analysis – 60 kW fuel cell power limit (3)

In Figure 13a the limiting of the fuel cell current is visible and the substitution of the missing portion with current from the battery. The speed of the motor appears in relation to the motor current, verifying the validity of the motor model operation.

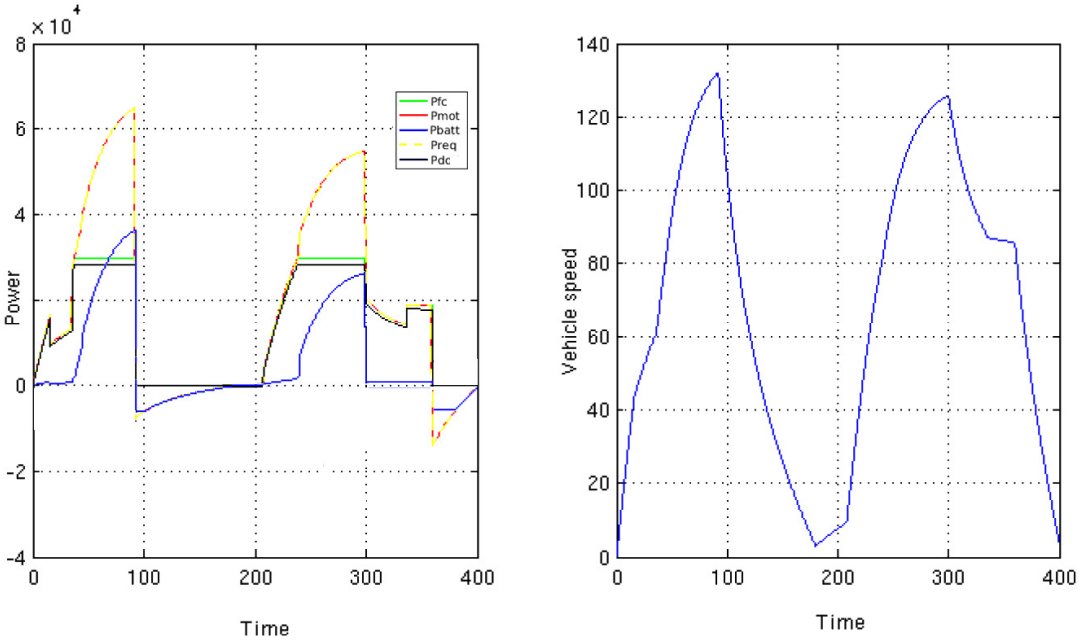


Figure 14: Sensitivity analysis – 30 kW fuel cell power limit (1)

In Figure 14a the limiting is noticeably more aggressive, leading to a big increase in the battery power but the vehicle speed still correlates with the torque requirements.

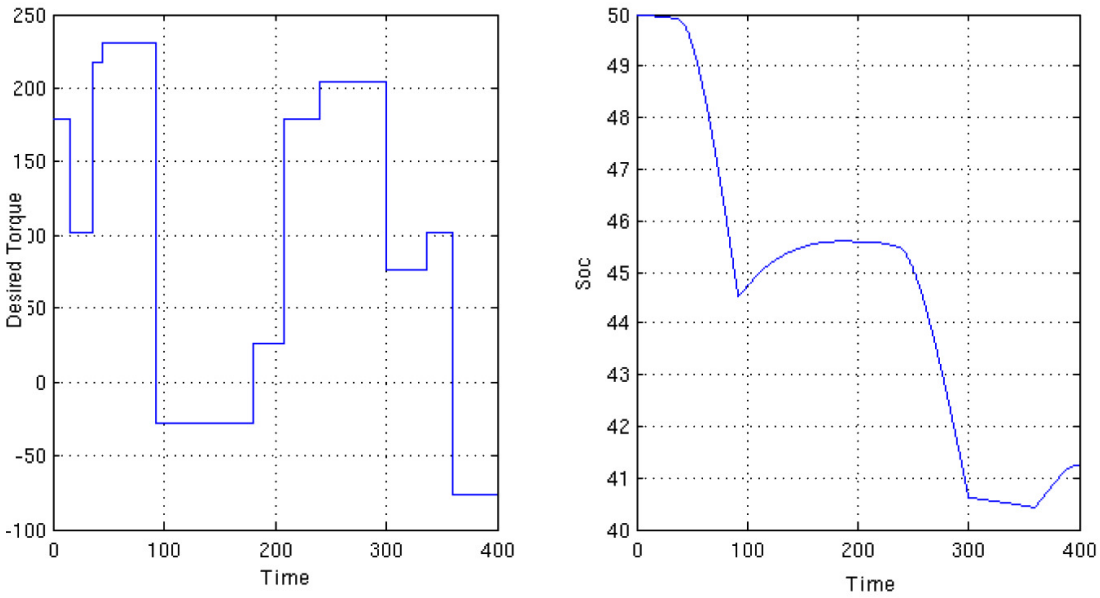


Figure 15: Sensitivity analysis – 30 kW fuel cell power limit (2)

In Figure 15b the decrease of the battery state of charge is even more apparent, with the harvested regenerative power now unable to bring the battery state of charge in pre operation levels.

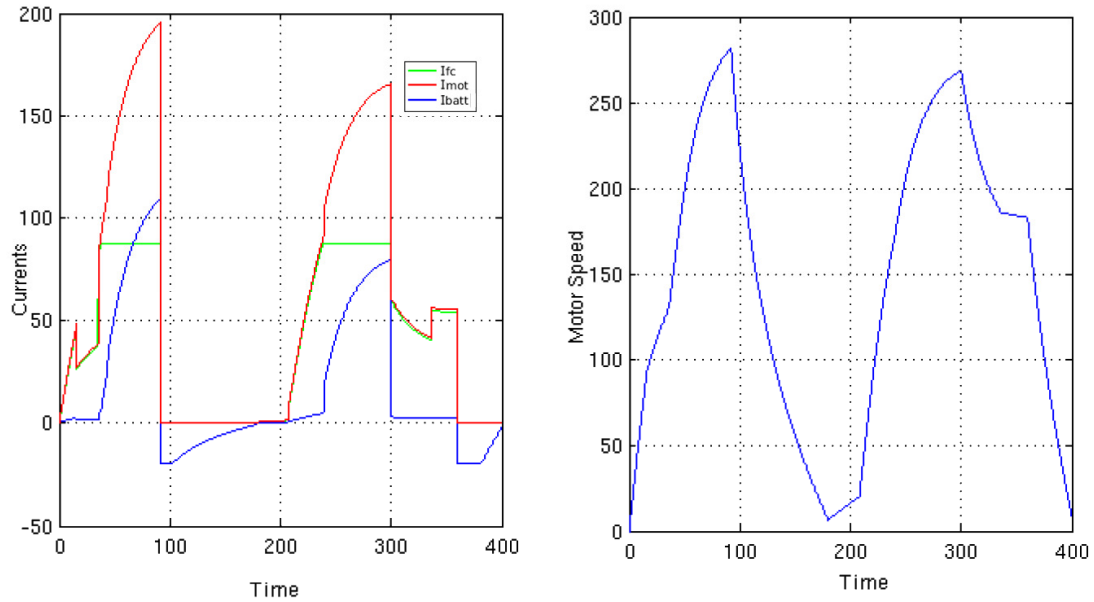


Figure 16: Sensitivity analysis – 30 kW fuel cell power limit (3)

Figure 16a presents the substantial increase in the battery current.

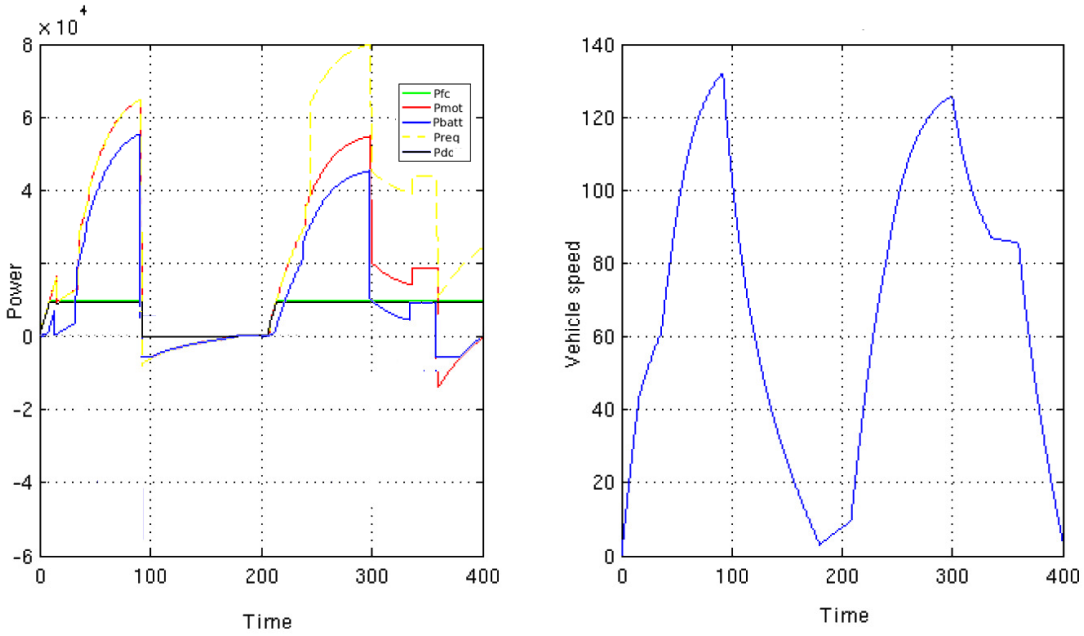


Figure 17: Sensitivity analysis – 10 kW fuel cell power limit (1)

In Figure 17a now can be clearly seen that nearly all of the required power is provided by the battery, with just a small portion filled in by the fuel cell, while the vehicle moves as expected.

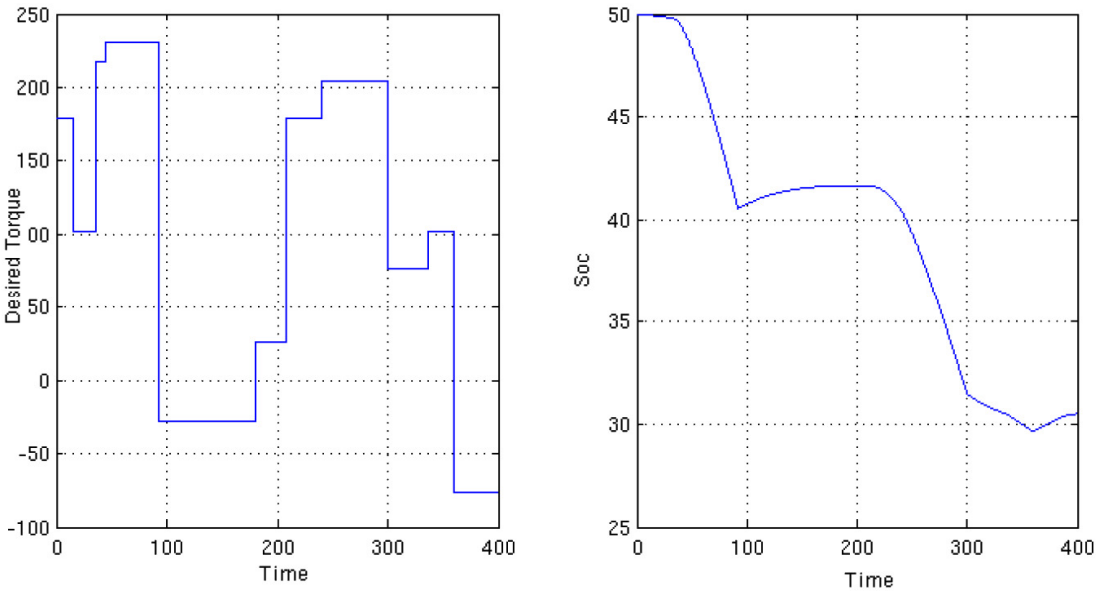


Figure 18: Sensitivity analysis – 10 kW fuel cell power limit (2)

In Figure 18b the immense reduction in battery state of charge is indisputable, with the value reaching as low as thirty percent, a value the can greatly reduce its lifetime.

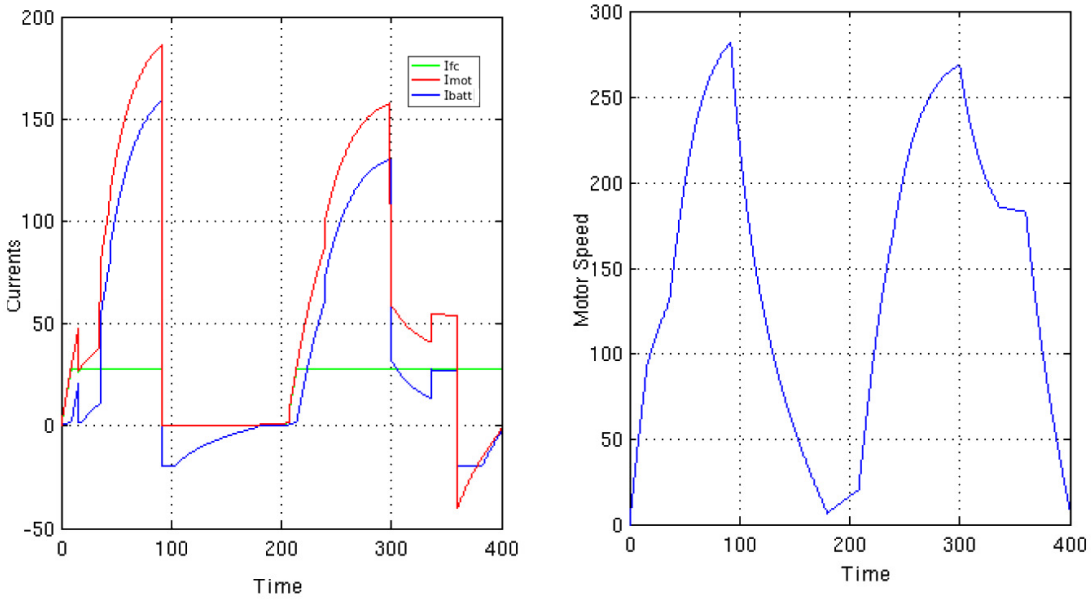


Figure 19: Sensitivity analysis – 10 kW fuel cell power limit (3)

In Figure 19a the battery current is greatly elevated, and the fuel cell current limited to a very low value. The speed of the motor is again as anticipated.

The results of this sensitivity analysis show that limiting the power that the fuel cell can provide has a direct result in the battery state of charge without affecting the movement of the vehicle because the requested power is provided. Thus the problem of power management can be studied and techniques to tackle the issue can be formulated.

# 5

# Heuristics Controller

This chapter deals with the formulation of the first control method assessed, the Heuristic Controller (finite state machine). After an introduction to the nature of operation of the controller, the results are presented.

## 5.1 Description of Operation and States

A simplistic approach to the energy management system is initially implemented in the form of a heuristics rule-based controller (finite state machine) with five states:

1. Discharging (SOC higher than desired $SOC_d$)
2. Discharging - maximum $I_b$ reached
3. Discharging - maximum $I_{fc}$ reached
4. Charging (SOC lower than desired $SOC_d$)
5. Charging - maximum $I_{fc}$ reached

The transition between the states occurs when a specific condition has been met as can be seen in the state diagram of the heuristic controller in Figure 20.

The controller has a fixed power split ratio between the two sources when discharging the battery and a charge mode during which the FC covers both the power demand of the user and the power required for battery charging.

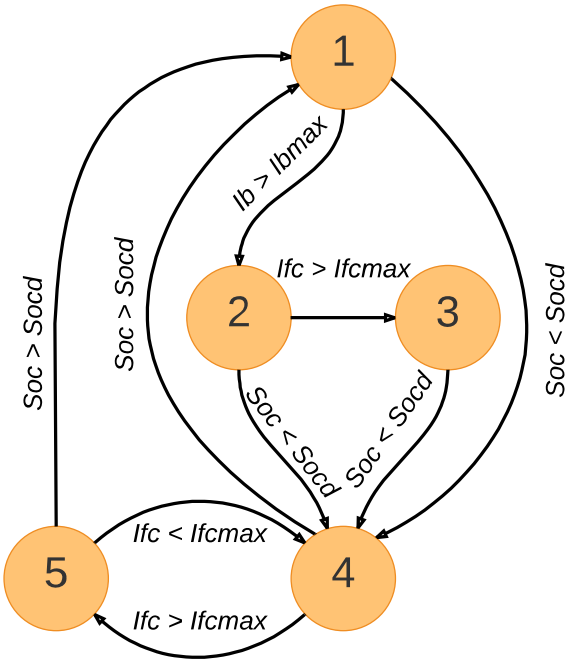


Figure 20: Heuristic controller state diagram

The performance of the heuristic controller was evaluated using a demanding driving cycle designed to demonstrate the response of the system in onerous situations such as abrupt accelerations and decelerations.

The duration of the simulation is 200 seconds with a simulation step of 1 second.

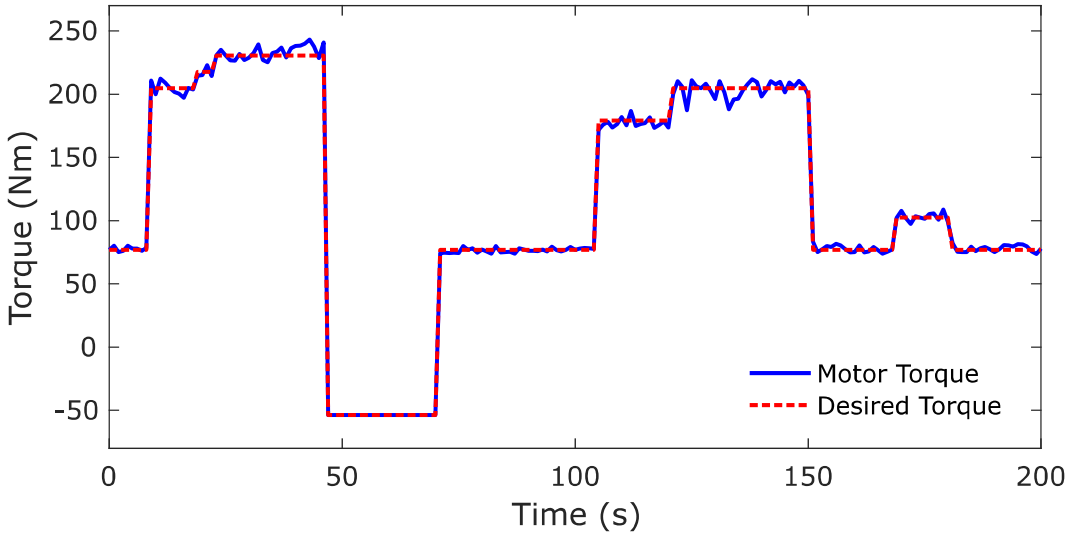


Figure 21: Heuristic controller – torque

The controller appears to provide the requested torque in a satisfying manner, both in steady state and in fast transients (abrupt accelerations and decelerations).

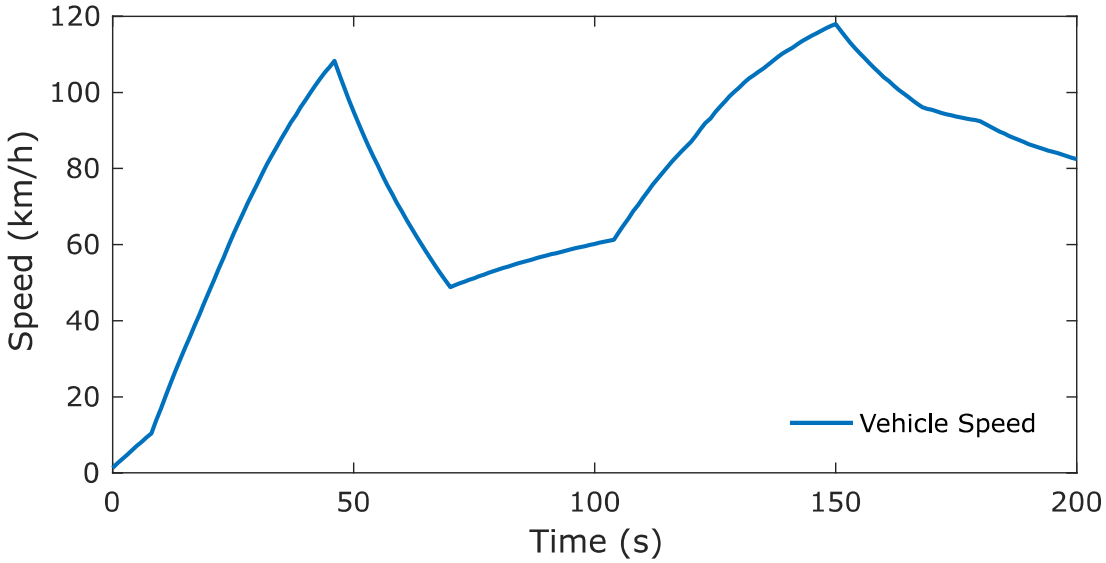

Figure 22: Heuristic controller – vehicle speed

The speed of the vehicle (Figure 22) varies in a smooth way, directly proportional to the torque provided by the motor.

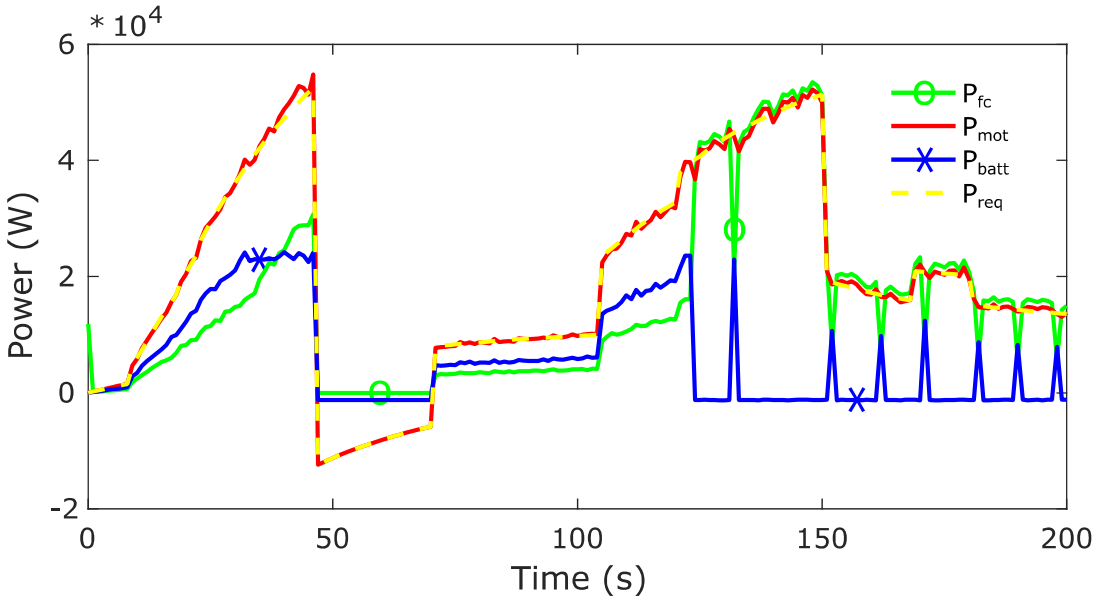

Figure 23: Heuristic controller – power

In Figure 23 the fixed power split of 60/40 (battery - FC) is evident with the controller being on the state of discharging (SOC > $SOC_d$). When enough power is drawn from the battery and the SOC reaches the desired value, the controller switches between two states (one and four) in a way that not only is inefficient, but puts the system under unnecessary stress. The effect of this drawback of the controller is also noticeable in Figure 24 as ripples on the SOC of the battery when it nears the desired value.

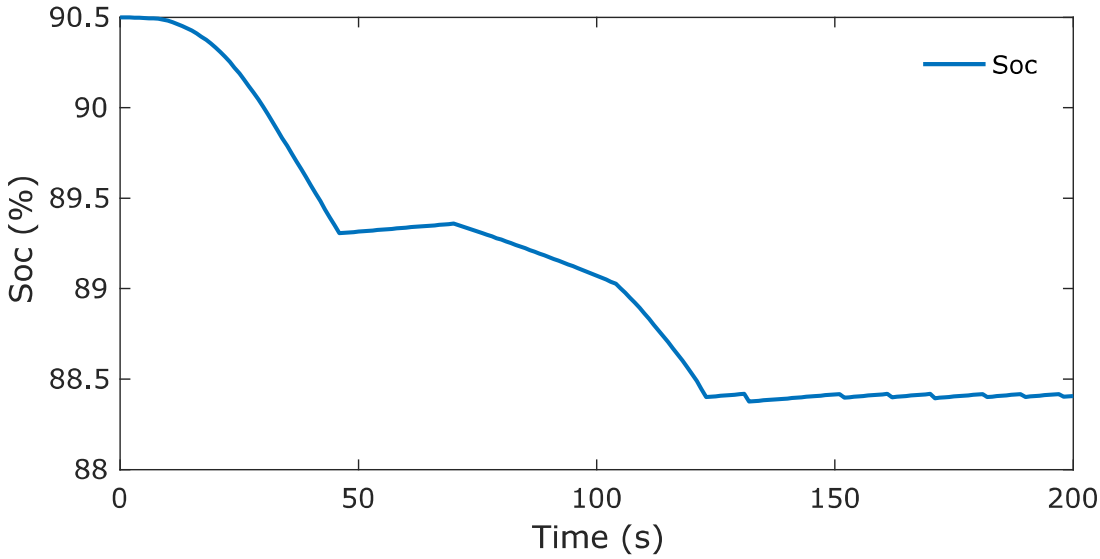

Figure 24: Heuristic controller – battery state of charge

Another major drawback for this approach is the inability of the controller to regulate the fuel and air flow rates of the fuel cell (Figure 25) to keep the excess ratios in the acceptable operation range, requiring extra controllers in order to be usable. Figure 26 depicts the lambda values as a result of the uncontrolled flow rates which indicate inefficient operation and high risk of FC membrane deterioration.

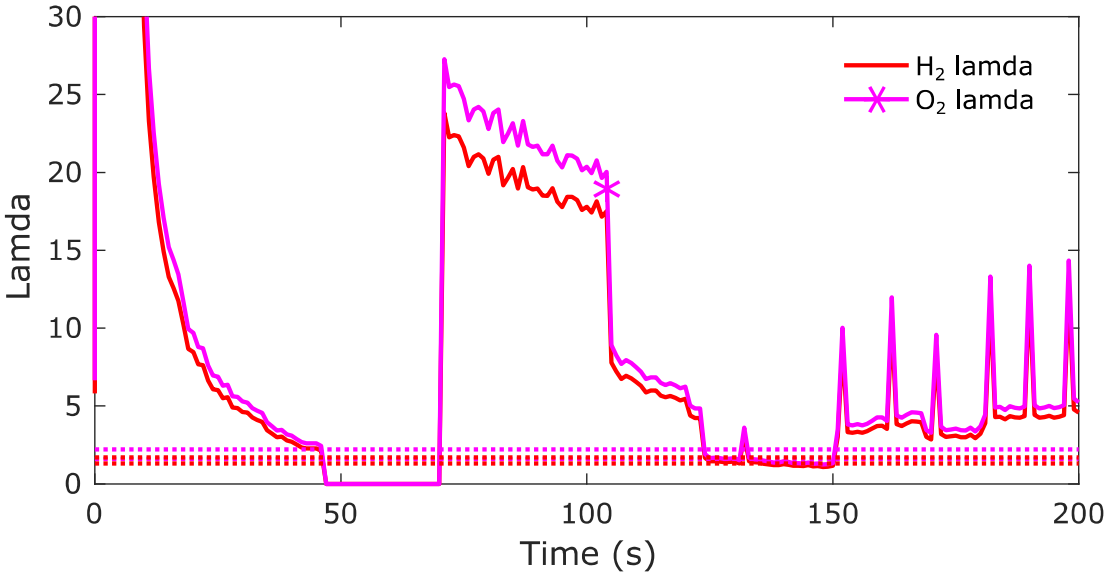

Figure 25: Heuristic controller – lambda values

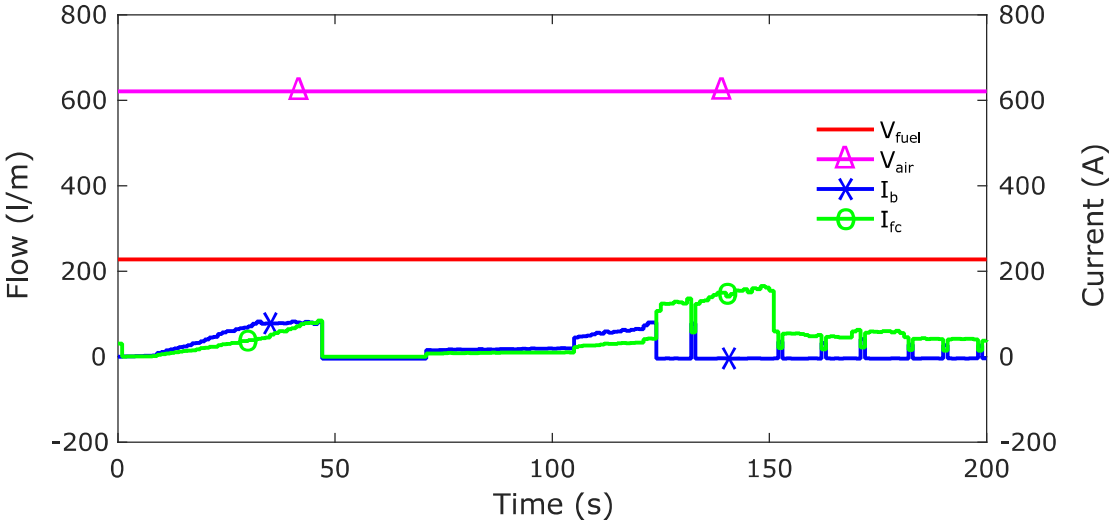

Figure 26: Heuristic controller – manipulated variables

Overall, the performance of the heuristic controller is deemed unsatisfying, not only because of the lack of optimality and unnecessary stress but also because of the inability that the heuristic controller presents in including the control of additional aspects of the system.

# 6

# Model Predictive Controller

This chapter deals with the description of the operation of a model predictive controller, the principles of operation and problem formulation, the optimization problem, and the adaptation of model predictive control methodology to this specific problem.

## 6.1 Introduction to Model Predictive Control

In order to fully cover the operational requirements of the system and implement the proposed control scheme, the need of a more advanced controller arises. The proposed control method is a model predictive controller.

Model predictive control (MPC) or receding horizon control (RHC) is considered as an advanced control method capable of providing on-line optimal operation for each timeslot while keeping in consideration future behavior of the system. It is part of a family of optimization-based control methods, which solves online an open loop finite horizon optimal control problem for the determination of the future control moves and is based on the fact that past and present control actions affect the future response of the system. The main objective is to obtain a control action by minimizing a quadratic cost function related to selected objectives or performance indices of the system. As the conditions of the system and the dynamics change and evolve through time, the optimization problem has to be solved online at consecutive sampling intervals. At each sampling time a finite horizon optimal control problem is solved over a prediction

horizon $T_p$, using the current state of the process as the initial state. The optimization yields an optimal control sequence $u_k$ ... $u_{k+Nc}$ over a control horizon $T_c$ and only the first control action $u_k$ for the current time is applied to the system. At the next time instant the horizon is shifted by one sampling interval and the optimization problem is resolved using the information of the new measurements acquired from the system [6]. The concept of receding horizon adds a feedback to the whole approach that enables the compensation of disturbances affecting the system or modeling inaccuracies. This methodology makes explicit use of a process model to optimize the predicted future behavior of the system. Thus, the first step in designing an MPC system is the development or selection of a suitable for control purposes mathematical model. Depending on the nature of the model, linear or nonlinear, we refer to MPC or Nonlinear MPC (NMPC) formulation. For the rest of this thesis we will use the NMPC approach as we are interested on nonlinear processes. A process model always includes some assumptions or simplifications with respect to the system which is represented, that may lead to minor inaccuracies. Also, the effect of disturbances to the process may add some extra uncertainty compared to the response of the developed model. Deviations of the model predictions from the actual process response are calculated at each sampling instance and considered as the error of the process model. This error defines a bias term which is used to correct future predictions and it is considered constant for the entire prediction horizon step.

The mathematical representation of the MPC algorithm subject to nonlinear inequality constraints *C(x)* is as follows:

$$\min_{u} J = \sum_{j=1}^{N_p}\left[(\hat{y}_{k+j} - y_{sp,k+j})^T\, Q\left(\hat{y}_{k+j} - y_{sp,k+j}\right)\right] +$$

$$\sum_{i=0}^{Nc-1} \Delta u_{k+l}^T R \Delta u_{k+l} \tag{35}$$

s.t.: $\dot{x} = f_d(x,u), \quad y = g(x,u)$ (36)

$$e_k = \left(y_{pred} - y_{meas}\right)_k, \hat{y}_{k+j} = y_{pred,k+j} + e_k \tag{37}$$

$$C(x) \leq 0 \tag{38}$$

The minimization of functional $J$ is subject to constraints on the manipulated $u$ and controlled $y$ variables. $y_{sp}$ denotes the desired reference trajectory, while $f_d$ are the differential equations and $g$ denotes the equations of the output variables. The difference $e_k$ between the measured variable $y_{meas}$ and the corresponding predicted value $y_{pred}$ at time instance $k$ is assumed to be constant for the entire number of time intervals $N_p$ of the prediction horizon $T_p$, $T_c$ denotes the control horizon reached through $N_c$ time intervals. Tuning parameters of the algorithm are the weight factors in the objective function ($Q$, $R$) and the length of the prediction and control horizon.

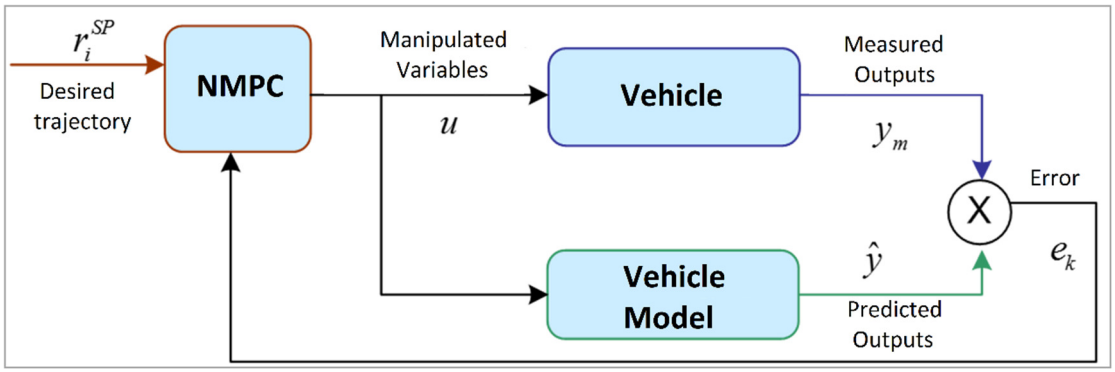


Figure 27: Model Predictive Control scheme

In order to simulate the "real" system to be controlled, the non-linear mathematical model is used but with various uncertainties introduced in the form of random value fluctuations, both in the state variables, the input variables but also in the measurements of the outputs by the controller.

## 6.2 Scope of the Optimization Problem

In both cases of MPC, linear and nonlinear, at the core of the control problem lies an optimization problem. The solution of this optimal control problem involves an optimization procedure that aims at the determination of the best solution for a given system considering physical and operating constraints. For this purpose various elements are necessary to formulate an optimization problem:

- A model that represents the behavior of the process and it is formulated by a set of equations and constraints.

- An objective function or performance index that defines a quantitative measure that need to be minimized, usually the tracking of a desired trajectory for the MPC case.
- A set of decision variables that are appropriately adjusted to satisfy the constraints and achieve the minimization of the predetermined objective function. These variables are the degrees of freedom of the system.

In order to systematically determine the optimal solution of the problem using these elements various methods and algorithms are available. Thus, the selection of the appropriate method is based on criteria derived by the nature of the system:

- Type of variables involved: discrete or continuous.
- Type of problem: differentiable or non-differentiable.
- Type of objective function and feasible region: convex or non-convex.

After the appropriate formulation of the optimization problem the rest of the MPC elements (e.g., control and prediction horizon, weights of terms in the objective etc., error calculation) are assembled and the integrated framework is ready to be used, initially for parameter tuning and subsequently for implementation at the process or for simulation purposes. In many cases and more specifically when a nonlinear formulation is involved, the solution of the optimization problem in each sampling instance is computationally demanding. To avoid computational delays and deterioration of the control performance, the optimization problem must be solved in a time period smaller than the sampling time interval of the system. Therefore, it is important to use a methodology that takes into consideration all the operating constraints which are imposed by the nature of the process into consideration.

The mathematical formulation of the optimization problem:

$$min\ J = \sum_{j=1}^{N_p} \left[ w_1 \left(T_{sp} - T\right)^2 + w_2 \left(1 + \frac{I_b}{|I_b|}\left(1 - e^{-|I_b|}\right) \frac{SOC_{des} - SOC}{SOC_{des} - SOC_{min}}\right)\right] \tag{39}$$

$$N_C = \frac{(T_c - T_k)}{\Delta t_c} \tag{40}$$

$$N_p = \frac{(T_p - T_k)}{\Delta t_p} \tag{41}$$

$$I_{fc\,min} \leq I_{fc\,k+j-1} \leq I_{fc\,max} \tag{42}$$

$$I_{b\,min} \leq I_{b\,k+j-1} \leq I_{b\,max} \tag{43}$$

$$V_{air\,min} \leq V_{air\,k+j-1} \leq V_{air\,max} \tag{44}$$

$$V_{fuel\,min} \leq V_{fuel\,k+j-1} \leq V_{fuel\,max} \tag{45}$$

$$C_1 = |1.5 - \lambda_{H2}| - 0.2 \tag{46}$$

$$C_2 = |1.9 - \lambda_{O2}| - 0.3 \tag{47}$$

Using equations (46),(47) the limiting of the excess ratios of the air and fuel is possible, in the form of a function that returns a negative value when the ratios are out of bounds. The two functions are depicted graphically in Figure 28.

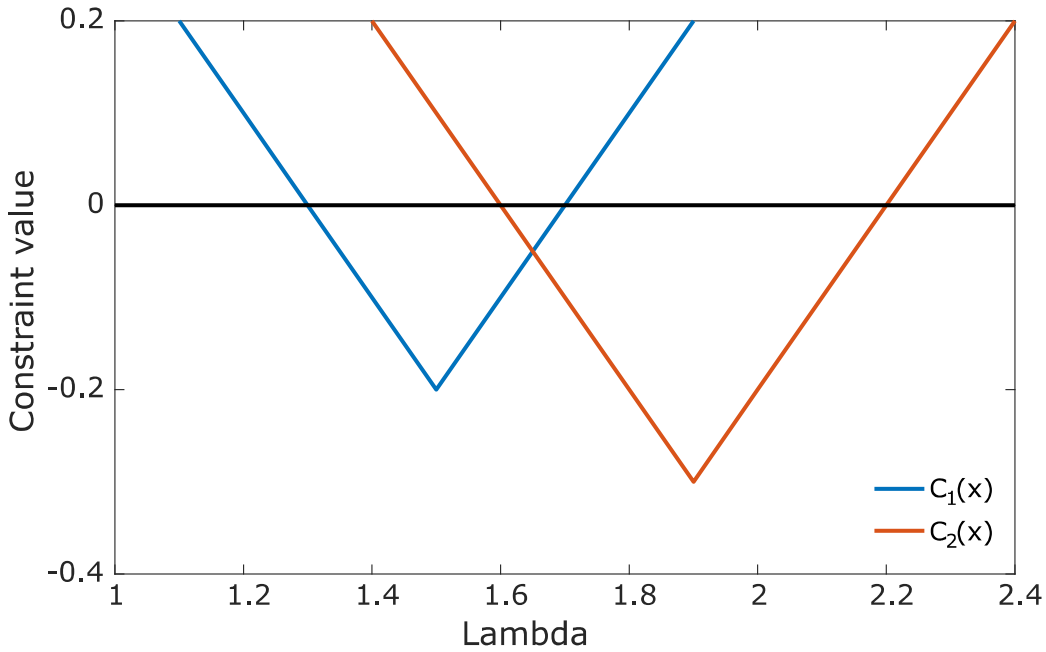


Figure 28: Lambda constraint functions

## 6.3 Cost Function & Sigmoid

$$J = w_1\left(T_{sp} - T\right) + w_2\left(1 + \frac{I_{batt}}{|I_{batt}|}\left(1 - e^{-|I_{batt}|}\right)\frac{Soc_d - SOC}{Soc_d - Soc_{min}}\right) \quad (48)$$

For this application, the cost function developed is comprised of two terms. The first ($T_{sp}$-$T$), as the optimizer tries to minimize the cost function has the effect of the controller increasing the power provided to the motor accordingly in order to match the torque requested by the user, because the term approaches zero as the provided torque matches the requested.

The second term is a sigmoid function whose slope depends on the difference of the battery SOC from a desired setpoint $SOC_d$ and its sign from the direction of the battery current. As such, the further below the SOC is from the desired value, the more the controller is encouraged to charge the battery by providing a negative current or utilizing the excess power when the battery SOC is higher than the setpoint. The effect of this term is that the battery tends to stay at the desired SOC and is used only when the FC cannot meet the power demand. A battery that is never fully charged guarantees that any power generated from braking will always be absorbed.

The two terms are weighted by their weights $w_1$ and $w_2$ which constitute two of the tuning parameters of the controller. Their value adjusts the impact that each term has on the optimization process; for example increasing $w_1$ makes the controller more devoted to provide the requested torque than keeping the battery SOC to the desired value. Figure 29 shows the sigmoid term for a desired SOC of 0.50 (50%) and different SOC values as a function of the battery current [22].

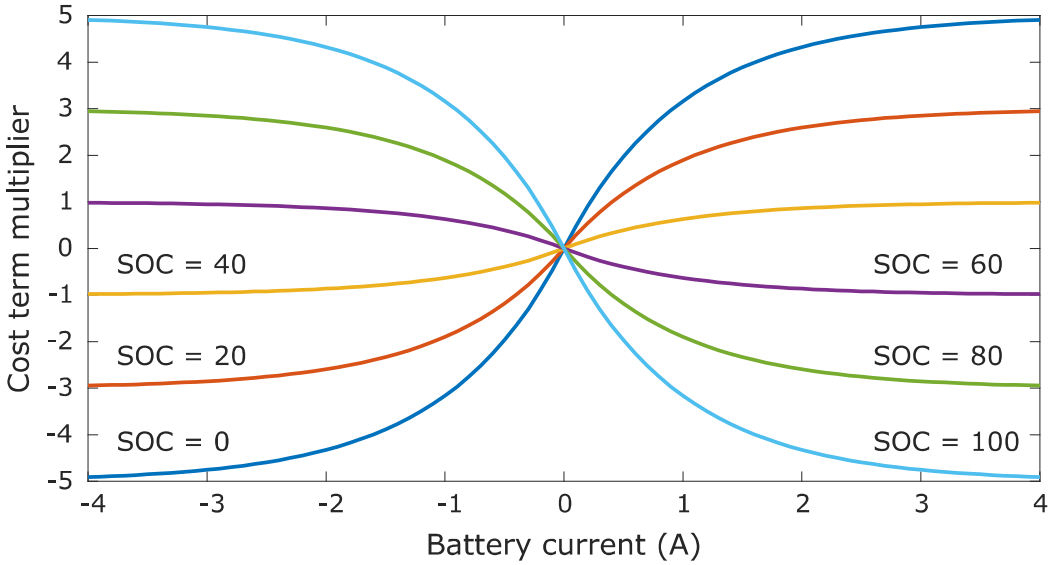

Figure 29: Sigmoid cost term for $SOC_d = 0.50$ (50%)

## 6.4 Solving the Optimization Problem

As the model of the system has been implemented in *MATLAB* environment, a variety of optimization solving algorithms can be tested which are available in the *Optimization Toolbox*.

The tool of choice is the *fmincon* solver, and the following algorithms have been evaluated:

- Interior Point
- Active Set
- Sequential Quadratic Programming

Of all the aforementioned algorithms, Interior Point showed the most promising results, being significantly more able to converge to an accepted solution for the specific problem.

In order to further improve the performance of the optimization solver, a multitude of solver options were changed. Most notably, the minimum change in variables for the finite-difference gradients was increased, the type of the finite differences was set to *central* which takes twice as many function evaluations but is more accurate, and the step termination tolerance was reduced.

## 6.5 Simulation Results

The performance of the proposed controller was validated using the same driving cycle as the heuristics controller. The duration of the simulation is again 200 seconds with a simulation step of 1 second, prediction horizon of 3 samples, control horizon of 1 sample, -4A – 80A battery current bounds, 0A – 347A FC current bounds, 95% as a desired SOC setpoint and lambda values constrained to 1.3 – 1.7 for the anode ($H_2$) and 1.6 – 2.2 for the cathode ($O_2$) as resulting from equations (46),(47). The controller satisfies the torque demand of the operator and given that the desired value for the SOC of the battery is higher than the starting SOC, the battery is only utilized when the FC cannot provide the requested power while staying in the desired operating conditions. The regenerative braking is also evident as a negative battery power in Figure 30 during deceleration and increased slope of battery SOC in Figure 33.

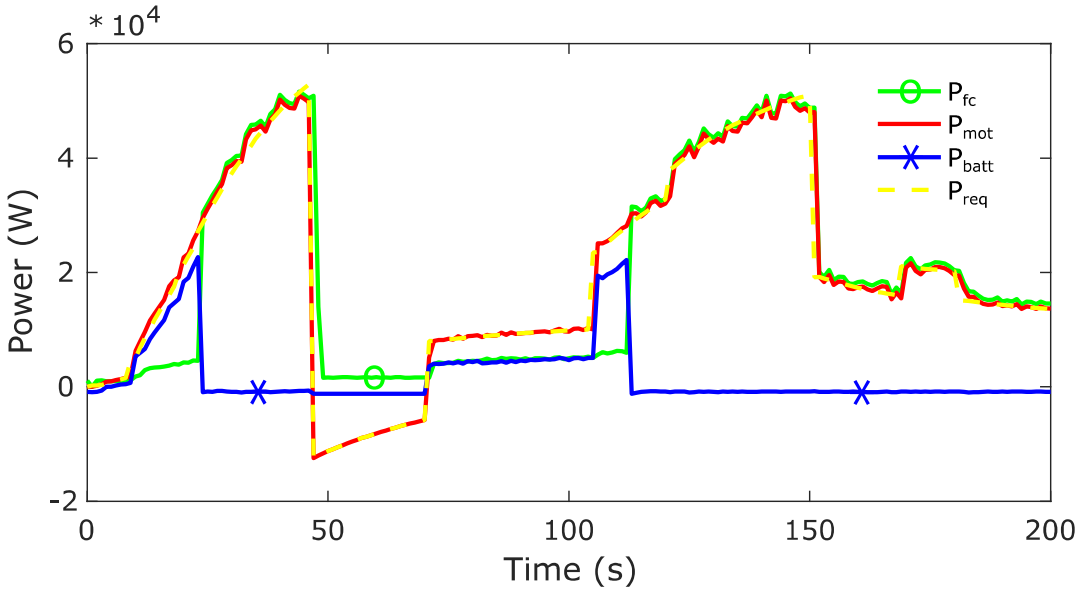


Figure 30: MPC controller – power

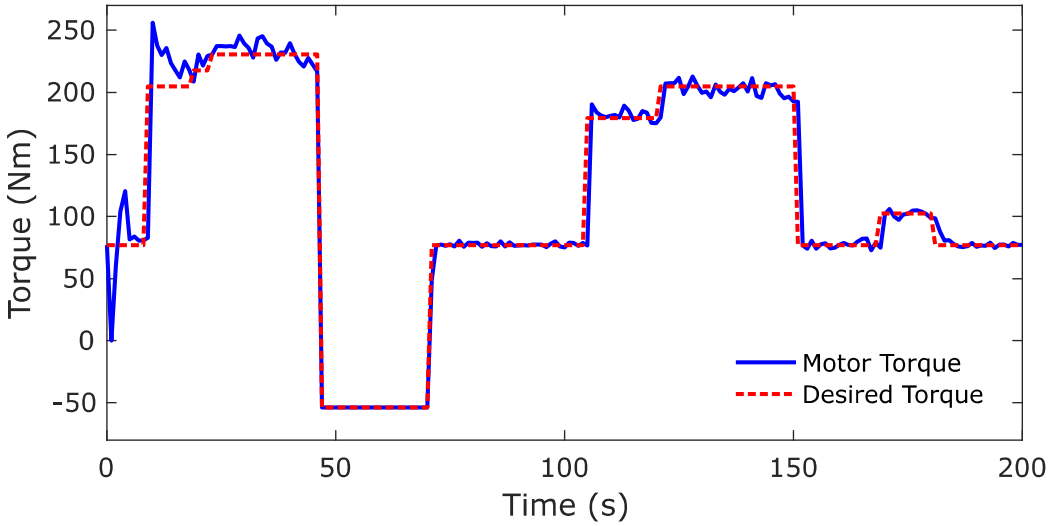

Figure 31: MPC controller – torque

The controller provides the user requested torque and is capable of following the desired trajectory both in steady state and in transient and abrupt variations (Figure 31).

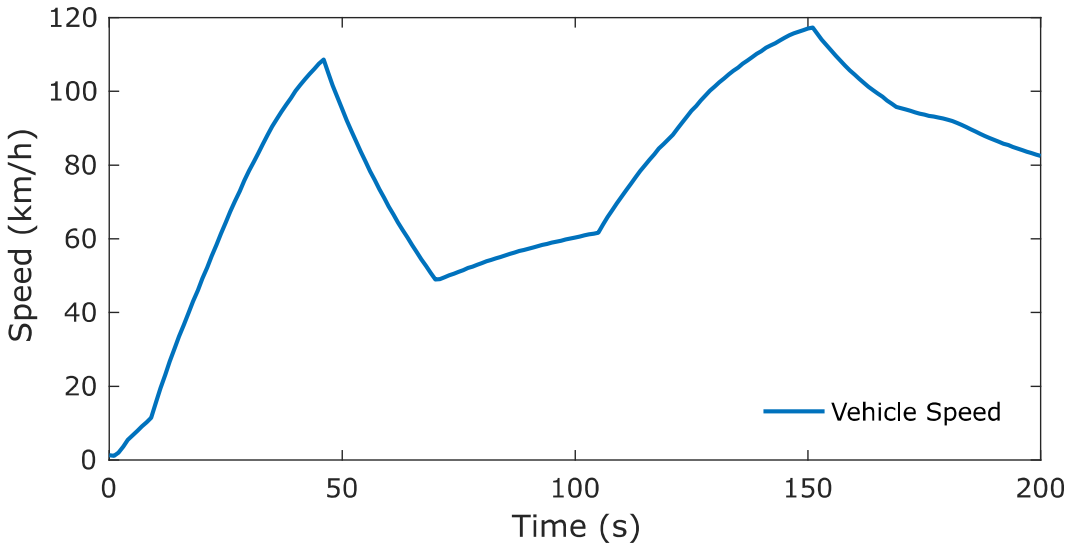

Figure 32: MPC controller – Vehicle speed

The speed of the vehicle (Figure 32) varies again in a smooth way, directly proportional to the torque provided by the motor.

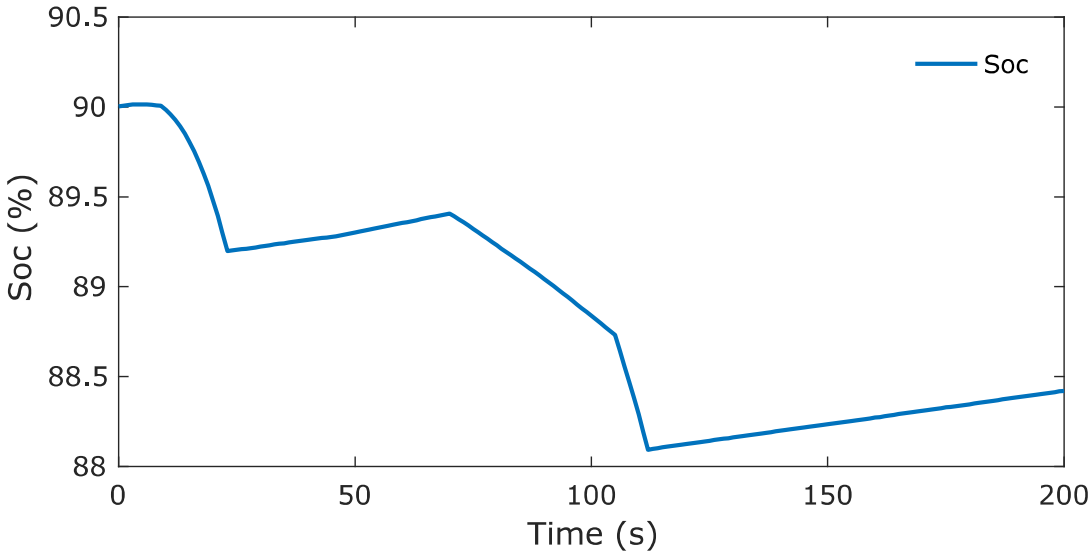

Figure 33: MPC controller – battery state of charge

In Figure 33 the areas where the battery is charging either from the fuel cell or the regenerative braking are evident together with the discharging when power is drawn from it.

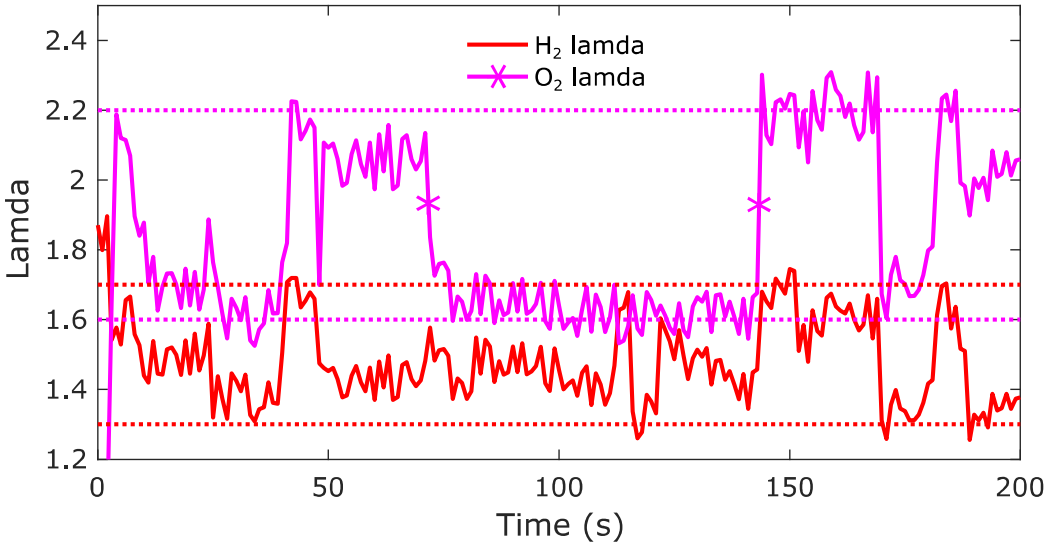

Figure 34: MPC controller – lambda values

In Figure 34 the reactant excess ratios are depicted, and the desired range for each is denoted by dotted lines. The ability of the controller to constrain the values within the specified range is evident, an action that ensures the protection of the fuel cell from membrane degradation and lifetime increase.

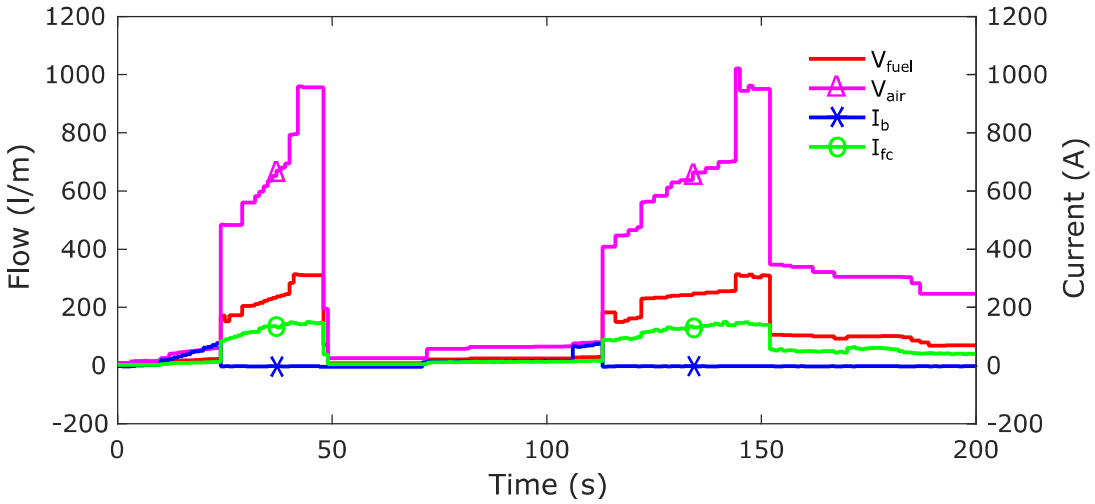

Figure 35: MPC controller – manipulated variables

Finally in Figure 35 the actions of the controller are presented (manipulated variables). The actions taken by the controller in order to contain the excess ratios within specification can be seen in the form of the trajectory of the reactant flow rates.

# 7

# Conclusions

In this thesis a dynamic, non-linear FCEV model was formulated along with its components, and an NMPC controller was developed capable of covering the operational requirements of the system. The integration of all control objectives in a single controller was presented and the performance was validated with driving cycle simulations. The response of the controller is deemed satisfying both in respect to the user's requests but also in the containment of the manipulated and controlled values within the desired operating range.

The fact that a non-linear model was used reassures the determination of the required values of the manipulated variables over a broad range of operational conditions and states and not only in a linearized area, and increases the effectiveness of the controller in the presence of unwanted disturbances.

With this application, the ability to employ the proposed control strategy to multivariable non-linear control problems with multiple objectives was verified.

## 7.1 Future Work

Various enhancements have been considered in order to fully utilize the potential of the developed framework such as:

1. Exploration of an FPGA implementation of the optimization formulation
2. Assess the behavior of different system topologies, e.g. with the addition of a supercapacitor power bank
3. Explore the use of an optimization solver that can be deployed to embedded systems e.g. multi-parametric MPC
4. Employ additional techniques that aid the achievement of global optimality such as route memory and route characteristics anticipation
5. Add more controlled and manipulated variables of the system, e.g. fuel cell stack temperature, compressor control

# 8

# References


[1] C. Bordons, M. A. Ridao, A. Pérez, A. Arce, and D. Marcos, "Model Predictive Control for power management in hybrid fuel cell vehicles," in *Vehicle Power and Propulsion Conference (VPPC), 2010 IEEE*, 2010, pp. 1–6.

[2] A. Arce, A. J. del Real, and C. Bordons, "MPC for battery/fuel cell hybrid vehicles including fuel cell dynamics and battery performance improvement," *J. Process Control*, vol. 19, no. 8, pp. 1289–1304, Sep. 2009.

[3] O. Tremblay, L.-A. Dessaint, and A.-I. Dekkiche, "A Generic Battery Model for the Dynamic Simulation of Hybrid Electric Vehicles," 2007, pp. 284–289.

[4] O. Tremblay, L.-A. Dessaint, and others, "A generic fuel cell model for the simulation of fuel cell vehicles," in *2009 IEEE Vehicle Power and Propulsion Conference*, 2009, pp. 1722–1729.

[5] C. Ziogou, D. Giaouris, C. Yfoulis, F. Stergiopoulos, S. Voutetakis, and S. Papadopoulou, "Behaviour Assessment of a Fuel Cell - Battery System Using a Supervisory Control Methodology Empowered by a Hybrid Timed Automaton (HTA)," in *Computer Aided Chemical Engineering*, vol. 37, Elsevier, 2015, pp. 2327–2332.

[6] C. Ziogou, S. Papadopoulou, M. C. Georgiadis, and S. Voutetakis, "On-line nonlinear model predictive control of a PEM fuel cell system," *J. Process Control*, vol. 23, no. 4, pp. 483–492, Apr. 2013.

[7] C. Ziogou, S. Voutetakis, S. Papadopoulou, and M. C. Georgiadis, "Modeling, simulation and experimental validation of a PEM fuel cell system," *Comput. Chem. Eng.*, vol. 35, no. 9, pp. 1886–1900, Sep. 2011.

[8] J. M. Correa, F. A. Farret, L. N. Canha, and M. G. Simoes, "An Electrochemical-Based Fuel-Cell Model Suitable for Electrical Engineering Automation Approach," *IEEE Trans. Ind. Electron.*, vol. 51, no. 5, pp. 1103–1112, Oct. 2004.

[9] J. T. Pukrushpan, H. Peng, and A. G. Stefanopoulou, "Control-Oriented Modeling and Analysis for Automotive Fuel Cell Systems," *J. Dyn. Syst. Meas. Control*, vol. 126, no. 1, p. 14, 2004.

[10] O. Tremblay and L.-A. Dessaint, "Experimental validation of a battery dynamic model for EV applications," *World Electr. Veh. J.*, vol. 3, no. 1, pp. 1–10, 2009.

[11] A. Jaafar, C. Turpin, X. Roboam, E. Bru, and O. Rallieres, “Energy management of a hybrid system based on a fuel cell and a Lithium Ion battery: Experimental tests and integrated optimal design,” *Math. Comput. Simul.*, vol. 131, pp. 21–37, Jan. 2017.
[12] P. Thounthong, S. Raël, and B. Davat, “Energy management of fuel cell/battery/supercapacitor hybrid power source for vehicle applications,” *J. Power Sources*, vol. 193, no. 1, pp. 376–385, Aug. 2009.
[13] A. M. Bassam, A. B. Phillips, S. R. Turnock, and P. A. Wilson, “An improved energy management strategy for a hybrid fuel cell/battery passenger vessel,” *Int. J. Hydrog. Energy*, vol. 41, no. 47, pp. 22453–22464, Dec. 2016.
[14] I. Lachhab and L. Krichen, “An improved energy management strategy for FC/UC hybrid electric vehicles propelled by motor-wheels,” *Int. J. Hydrog. Energy*, vol. 39, no. 1, pp. 571–581, Jan. 2014.
[15] H. Hemi, J. Ghouili, and A. Cheriti, “A real time fuzzy logic power management strategy for a fuel cell vehicle,” *Energy Convers. Manag.*, vol. 80, pp. 63–70, Apr. 2014.
[16] H. Hemi, J. Ghouili, and A. Cheriti, “Combination of Markov chain and optimal control solved by Pontryagin’s Minimum Principle for a fuel cell/supercapacitor vehicle,” *Energy Convers. Manag.*, vol. 91, pp. 387–393, Feb. 2015.
[17] J. Bernard, S. Delprat, T. M. Guerra, and F. N. Büchi, “Fuel efficient power management strategy for fuel cell hybrid powertrains,” *Control Eng. Pract.*, vol. 18, no. 4, pp. 408–417, 2010.
[18] W.-S. Lin and C.-H. Zheng, “Energy management of a fuel cell/ultracapacitor hybrid power system using an adaptive optimal-control method,” *J. Power Sources*, vol. 196, no. 6, pp. 3280–3289, Mar. 2011.
[19] K. Ettihir, L. Boulon, and K. Agbossou, “Optimization-based energy management strategy for a fuel cell/battery hybrid power system,” *Appl. Energy*, vol. 163, pp. 142–153, Feb. 2016.
[20] A. Vahidi, A. Stefanopoulou, and H. Peng, “Current Management in a Hybrid Fuel Cell Power System: A Model-Predictive Control Approach,” *IEEE Trans. Control Syst. Technol.*, vol. 14, no. 6, pp. 1047–1057, Nov. 2006.
[21] W. Greenwell and A. Vahidi, “Predictive Control of Voltage and Current in a Fuel Cell-Ultracapacitor Hybrid,” *IEEE Trans. Ind. Electron.*, vol. 57, no. 6, pp. 1954–1963, Jun. 2010.
[22] O. Laldin, M. Moshirvaziri, and O. Trescases, “Predictive Algorithm for Optimizing Power Flow in Hybrid Ultracapacitor/Battery Storage Systems for Light Electric Vehicles,” *IEEE Trans. Power Electron.*, vol. 28, no. 8, pp. 3882–3895, Aug. 2013.